RESEARCH ARTICLE

A zebrafish embryo screen utilizing gastrulation identifies the HTR2C inhibitor pizotifen as a suppressor of EMT-mediated metastasis

Joji Nakayama[1,2,3,4]*, Lora Tan[1], Yan Li[1], Boon Cher Goh[2], Shu Wang[1,5], Hideki Makinoshima[3,6], Zhiyuan Gong[1]*

[1]Department of Biological Science, National University of Singapore, Singapore, Singapore; [2]Cancer Science Institute of Singapore, National University of Singapore, Singapore, Singapore; [3]Tsuruoka Metabolomics Laboratory, National Cancer Center, Tsuruoka, Japan; [4]Shonai Regional Industry Promotion Center, Tsuruoka, Japan; [5]Institute of Bioengineering and Nanotechnology, Singapore, Singapore; [6]Division of Translational Research, Exploratory Oncology Research and Clinical Trial Center, National Cancer Center, Kashiwa, Japan

Abstract Metastasis is responsible for approximately 90% of cancer-associated mortality but few models exist that allow for rapid and effective screening of anti-metastasis drugs. Current mouse models of metastasis are too expensive and time consuming to use for rapid and high-throughput screening. Therefore, we created a unique screening concept utilizing conserved mechanisms between zebrafish gastrulation and cancer metastasis for identification of potential anti-metastatic drugs. We hypothesized that small chemicals that interrupt zebrafish gastrulation might also suppress metastatic progression of cancer cells and developed a phenotype-based chemical screen to test the hypothesis. The screen used epiboly, the first morphogenetic movement in gastrulation, as a marker and enabled 100 chemicals to be tested in 5 hr. The screen tested 1280 FDA-approved drugs and identified pizotifen, an antagonist for serotonin receptor 2C (HTR2C) as an epiboly-interrupting drug. Pharmacological and genetic inhibition of HTR2C suppressed metastatic progression in a mouse model. Blocking HTR2C with pizotifen restored epithelial properties to metastatic cells through inhibition of Wnt signaling. In contrast, HTR2C induced epithelial-to-mesenchymal transition through activation of Wnt signaling and promoted metastatic dissemination of human cancer cells in a zebrafish xenotransplantation model. Taken together, our concept offers a novel platform for discovery of anti-metastasis drugs.

***For correspondence:**
zmetastasis@gmail.com (JN);
dbsgzy@nus.edu.sg (ZG)

Competing interest: The authors declare that no competing interests exist.

Funding: See page 26

Preprinted: 05 March 2021
Received: 07 May 2021
Accepted: 17 December 2021
Published: 17 December 2021

Reviewing Editor: Yasuhito Shimada, Mie University, Japan

Editor's evaluation

We are so impressed with this new and ambitious concept for chemical screening using zebrafish embryos to find a novel anti-metastasis drug, Pizotifen. We hope many researchers will use this screening system for anti-cancer drug discovery.

Introduction

Metastasis, a leading contributor to the morbidity of cancer patients, occurs through multiple steps: invasion, intravasation, extravasation, colonization, and metastatic tumor formation (***Nguyen et al., 2009***; ***Welch and Hurst, 2019***; ***Chaffer and Weinberg, 2011***). The physical translocation of cancer

cells is an initial step of metastasis and molecular mechanisms of it involve cell motility, the breakdown of local basement membrane, loss of cell polarity, acquisition of stem cell-like properties, and epithelial-to-mesenchymal transition (EMT) (***Tsai and Yang, 2013***; ***Lu and Kang, 2019***). These cell-biological phenomena are also observed during vertebrate gastrulation in that evolutionarily conserved morphogenetic movements of epiboly, internalization, convergence, and extension progress (***Solnica-Krezel, 2005***). In zebrafish, the first morphogenetic movement, epiboly, is initiated at approximately 4 hr post fertilization (hpf) to move cells from the animal pole to eventually engulf the entire yolk cell by 10 hpf (***Latimer and Jessen, 2010***; ***Solnica-Krezel, 2006***). The embryonic cell movements are governed by the molecular mechanisms that are partially shared in metastatic cell dissemination.

At least 50 common genes were shown to be involved in both metastasis and gastrulation progression: Knockdown of these genes in *Xenopus* or zebrafish induced gastrulation defects; conversely, overexpression of these genes conferred metastatic potential on cancer cells and knockdown of these genes suppressed metastasis (***Yang and Weinberg, 2008***; ***Dongre and Weinberg, 2019***; ***Thiery et al., 2009***; ***Nieto et al., 2016***; ***Table 1***). This evidence led us to hypothesize that small molecules that interrupt zebrafish gastrulation may suppress metastatic progression of human cancer cells.

Here, we report a unique screening concept based on the hypothesis. Pizotifen, an antagonist for HTR2C, was identified from the screen as a 'hit' that interrupted zebrafish gastrulation. A mouse model of metastasis confirmed pharmacological and genetic inhibition of HTR2C suppressed metastatic progression. Moreover, HTR2C induced EMT and promoted metastatic dissemination of non-metastatic cancer cells in a zebrafish xenotransplantation model. These results demonstrated that this concept could offer a novel high-throughput platform for discovery of anti-metastasis drugs and can be converted to a chemical genetic screening platform.

Results

Small molecules interrupting epiboly of zebrafish have a potential to suppress metastatic progression of human cancer cells

Before performing a screening assay, we validated a core of our concept through comparing the genes expressed in zebrafish gastrulation with the genes which expressed in EMT-mediated metastasis. Gene set enrichment analysis (GSEA) demonstrated that 50%-epiboly, shield, and 75%-epiboly stage of zebrafish embryos expressed the genes which promote EMT-mediated metastasis: EMT induction, TGF-β signaling, wnt/β-catenin signaling, Notch signaling (***Figure 1—figure supplement 1***).

We further conducted preliminary experiments to test the hypothesis. First, we examined whether hindering the molecular function of reported genes, whose knockdown induced gastrulation defects in zebrafish, might suppress cell motility and invasion of cancer cells. We chose protein arginine methyltransferase 1 (PRMT1) and cytochrome P450 family 11 (CYP11A1), both of whose knockdown induced gastrulation defects in zebrafish but whose involvement in metastatic progression is unclear (***Tsai et al., 2011***; ***Hsu et al., 2006***). Elevated expression of PRMT1 and CYP11A1 was observed in highly metastatic human breast cancer cell lines and knockdown of these genes through RNA interference suppressed the motility and invasion of MDA-MB-231 cells without affecting their viability (***Figure 1—figure supplement 2A-C***).

Next, we conducted an inverse examination of whether chemicals which were reported to suppress metastatic dissemination of cancer cells could interrupt epiboly progression of zebrafish embryos. Niclosamide and vinpocetine are reported to suppress metastatic progression (***Weinbach and Garbus, 1969***; ***Sack et al., 2011***; ***Huang et al., 2012***; ***Szilágyi et al., 2005***). Either niclosamide- or vinpocetine-treated zebrafish embryos showed complete arrest at very early stages or severe delay in epiboly progression, respectively (***Figure 1—figure supplement 2D***).

These results suggest that epiboly could serve as a marker for this screening assay and epiboly-interrupting drugs that are identified through this screening could have the potential to suppress metastatic progression of human cancer cells.

Table 1. A list of the genes that are involved between gastrulation and metastasis progression.

A list of the 50 genes that play essential role in governing both metastasis and gastrulation progression. The gastrulation defects in *Xenopus* or zebrafish that are induced by knockdown of each of these genes were indicated. The molecular mechanism in metastasis that is inhibited by knockdown of each of the same genes was indicated.

Genes	**Gastrulation defects**	**Ref**	**Effects in metastasis**	**Ref**
BMP	Convergence and extension	***Kondo, 2007***	EMT	***Katsuno et al., 2008***
WNT	Convergence and extension	***Tada and Smith, 2000***	Migration and invasion	***Vincan and Barker, 2008***
FGF	Convergence and extension	***Yang et al., 2002***	Invision	***Nomura et al., 2008***
EGF	Epiboly	***Song et al., 2013***	Migration	***Lu et al., 2001***
PDGF	Convergence and extension	***Damm and Winklbauer, 2011***	EMT	***Jechlinger et al., 2006***
CXCL12	Migration of endodermal cells	***Mizoguchi et al., 2008***	Migration and invasion	***Shen et al., 2013***
CXCR4	Migration of endodermal cells	***Mizoguchi et al., 2008***	Migration and invasion	***Shen et al., 2013***
PIK3CA	Convergence and extension	***Montero et al., 2003***	Migration and invasion	***Wander et al., 2013***
YES	Epiboly	***Tsai et al., 2005***	Migration	***Barraclough et al., 2007***
FYN	Epiboly	***Sharma et al., 2005***	Migration and invasion	***Yadav and Denning, 2011***
MAPK1	Epiboly	***Krens et al., 2008***	Migration	***Radtke et al., 2013***
SHP2	Convergence and extension	***Jopling et al., 2007***	Migration	***Wang et al., 2005***
SNAI1	Convergence and extension	***Ip and Gridley, 2002***	EMT	***Batlle et al., 2000***
SNAI2	Mesoderm and neural crest formation	***Shi et al., 2011***	EMT	***Medici et al., 2008***
TWIST1	Mesoderm formation	***Castanon and Baylies, 2002***	EMT	***Yang et al., 2004***
TBXT	Convergence and extension	***Tada and Smith, 2000***	EMT	***Fernando et al., 2010***
ZEB1	Epiboly	***Vannier et al., 2013***	EMT	***Spaderna et al., 2008***
GSC	Mesodermal patterning	***Sander et al., 2007***	EMT	***Hartwell et al., 2006***
FOXC2	Unclear, defects in gastrulation	***Wilm et al., 2004***	EMT	***Mani et al., 2007***

Table 1 continued on next page

Table 1 continued

Genes	Gastrulation defects	Ref	Effects in metastasis	Ref
STAT3	Convergence and extension	**Miyagi et al., 2004**	Migration	**Abdulghani et al., 2008**
POU5F1	Epiboly	**Lachnit et al., 2008**	EMT	**Dai et al., 2013**
EZH2	Unclear, defects in gastrulation	**O'Carroll et al., 2001**	Invasion	**Ren et al., 2012**
EHMT2	Defects in neurogenesis	**Lin et al., 2005**	Migration and invasion	**Chen et al., 2010**
BMI1	Defects in skeleton formation	**van der Lugt et al., 1994**	EMT	**Guo et al., 2011**
RHOA	Convergence and extension	**Zhu et al., 2006**	Migration and invasion	**Yoshioka et al., 1999**
CDC42	Convergence and extension	**Choi and Han, 2002**	Migration and invasion	**Reymond et al., 2012**
RAC1	Convergence and extension	**Habas et al., 2003**	Migration and invasion	**Vega and Ridley, 2008**
ROCK2	Convergence and extension	**Marlow et al., 2002**	Migration and invasion	**Itoh et al., 1999**
PAR1	Convergence and extension	**Kusakabe and Nishida, 2004**	Migration	**Shi et al., 2004**
PRKCI	Convergence and extension	**Kusakabe and Nishida, 2004**	EMT	**Gunaratne et al., 2013**
CAP1	Convergence and extension	**Seifert et al., 2009**	Migration	**Yamazaki et al., 2009**
EZR	Epiboly	**Link et al., 2006**	Migration	**Khanna et al., 2004**
EPCAM	Epiboly	**Slanchev et al., 2009**	Migration and invasion	**Ni et al., 2012**
ITGB1/ ITA5	Mesodermal migration	**Skalski et al., 1998**	Migration and invasion	**Felding-Habermann, 2003**
FN1	Convergence and extension	**Marsden and DeSimone, 2003**	Invasion	**Malik et al., 2010**
HAS2	Dorsal migration of lateral cells	**Bakkers et al., 2004**	Invasion	**Kim et al., 2004**
MMP14	Convergence and extension	**Coyle et al., 2008**	Invasion	**Perentes et al., 2011**
COX1	Epiboly	**Cha et al., 2006**	Invasion	**Kundu and Fulton, 2002**
PTGES	Convergence and extension	**Speirs et al., 2010**	Invasion	**Wang and Dubois, 2006**
SLC39A6	Anterior migration	**Yamashita et al., 2004**	EMT	**Lue et al., 2011**
GNA12 /13	Convergence and extension	**Lin et al., 2005**	Migration and invasion	**Yagi et al., 2011**

Table 1 continued on next page

Table 1 continued

Genes	Gastrulation defects	Ref	Effects in metastasis	Ref
OGT	Epiboly	**Webster et al., 2009**	Migration and invasion	**Lynch et al., 2012**
CCN1	Cell movement	**Latinkic et al., 2003**	Migration and invasion	**Lin et al., 2012**
TRPM7	Convergence and extension	**Liu et al., 2011**	Migration	**Middelbeek et al., 2012**
MAPKAPK2	Epiboly	**Holloway et al., 2009**	Migration	**Kumar et al., 2010**
B4GALT1	Convergence and extension	**Machingo et al., 2006**	Invasion	**Zhu et al., 2005**
IER2	Convergence and extension	**Hong et al., 2011**	Migration	**Neeb et al., 2012**
TIP1	Convergence and extension	**Besser et al., 2007**	Migration and invasion	**Han et al., 2012**
PAK5	Convergence and extension	**Faure et al., 2005**	Migration	**Gong et al., 2009**
MARCKS	Convergence and extension	**Iioka et al., 2004**	Migration and invasion	**Rombouts et al., 2013**

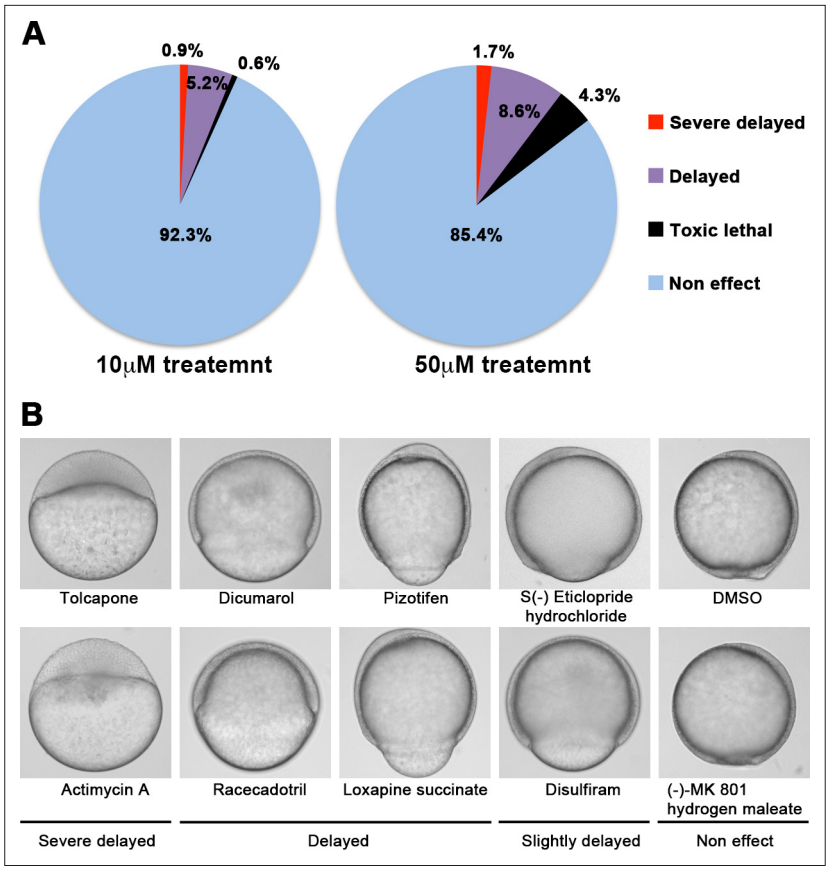

Figure 1. A chemical screen for identification of epiboly-interrupting drugs. (**A**) Cumulative results of the chemical screen in which each drug was used at either 10 μM (left) or 50 μM (right) concentrations. 1280 FDA, EMA, or other agencies-approved drugs were subjected to this screening. Positive 'hit' drugs were those that interrupted epiboly progression. (**B**) Representative samples of the embryos that were treated with indicated drugs.

The online version of this article includes the following figure supplement(s) for figure 1:

Figure supplement 1. Gene expression profiles obtained from zebrafish embryos at either 50%-epiboly (top left), shield (top right), or 75%-epiboly stage (bottom left) were analyzed based on the hallmark gene sets derived from the Molecular Signatures Database (MSigDB) (***Liberzon et al., 2015***).

Figure supplement 2. Epiboly could serve as a marker for this screening.

132 FDA-approved drugs induced delayed in epiboly of zebrafish embryos

We screened 1280 FDA, EMA, or other agencies-approved drugs (Prestwick, Inc) in our zebrafish assay. The screening showed that 0.9% (12/1280) of the drugs, including antimycin A and tolcapone, induced severe or complete arrest of embryonic cell movement when embryos were treated with 10 μM. 5.2% (66/1280) of the drugs, such as dicumarol, racecadotril, pizotifen, and S(-)eticlopride hydrochloride, induced either delayed epiboly or interrupted epiboly of the embryos. 93.3% (1194/1280) of drugs have no effect on epiboly progression of the embryos. 0.6% (8/1280) of drugs induced toxic lethality. Epiboly progression was affected more severely when embryos were treated with 50 μM; 1.7% (22/1280) of the drugs induced severe or complete arrest of it. 8.6% (110/1280) of the drugs induced either delayed epiboly or interrupt epiboly of the embryos. 4.3% (55/1280) of drugs induced a toxic lethality (***Figure 1A and B***, ***Table 2***). Among the epiboly-interrupting drugs, several drugs have already been reported to inhibit metastasis-related molecular mechanisms: adrenosterone or zardaverine, which target HSD11β1 or PDE3 and -4, respectively, are reported to inhibit EMT (***Nakayama et al., 2020***; ***Kolosionek et al., 2009***); racecadotril, which targets enkephalinase, is reported to confer metastatic potential on colon cancer cell (***Sasaki et al., 2014***); and disulfiram, which targets ALDH (aldehyde dehydrogenase), is reported to confer stem-like properties on

Table 2. A list of the drugs that interfere with epiboly progression in zebrafish.
Related to ***Figure 1***. A list of positive 'hit' drugs that interfered with epiboly progression. Gastrulation defects or status of each of the zebrafish embryos that were treated with either 10 or 50 μM concentrations are indicated.

Chemical name	Chemical formula	Effect of 10 **μM**	Effect of 50 **μM**
Acitretin	$C_{21}H_{26}O_3$	Delayed	Delayed
Adrenosterone	$C_{19}H_{24}O_3$	Delayed	Delayed
Albendazole	$C_{12}H_{15}N_3O_2S$	Severe delayed	Severe delayed
Alfadolone acetate	$C_{23}H_{34}O_5$	Delayed	Delayed
Alfaxalone	$C_{21}H_{32}O_3$	Delayed	Delayed
Alprostadil	$C_{20}H_{34}O_5$	Delayed	Delayed
Altrenogest	$C_{21}H_{26}O_2$	Slightly delayed	Delayed
Ampiroxicam	$C_{20}H_{21}N_3O_7S$	Non-effect	Delayed
Anethole-trithione	$C_{10}H_{8O}S_3$	Delayed	Delayed
Antimycin A	$C_{28}H_{40}N_2O_9$	Delayed	Delayed
Avobenzone	$C_{20}H_{22}O_3$	Delayed	Delayed
Benzoxiquine	$C_{16}H_{11}NO_2$	Non-effect	Delayed
Bosentan	$C_{27}H_{29}N_5O_6S$	Delayed	Delayed
Butoconazole nitrate	$C_{19}H_{18}C_{l3}N_3O_3S$	Delayed	Toxic lethal
Camptothecine (S,+)	$C_{20}H_{16}N_2O_4$	Severe delayed	Severe delayed
Carbenoxolone disodium salt	$C_{34}H_{48}Na_2O_7$	Delayed	Toxic lethal
Carmofur	$C_{11}H_{16}FN_3O_3$	Slightly delayed	Delayed
Carprofen	$C_{15}H_{12}ClNO_2$	Severe delayed	Toxic lethal
Cefdinir	$C_{14}H_{13}N_5O_5S_2$	Delayed	Delayed
Celecoxib	$C_{17}H_{14}F_3N_3O_2S$	Delayed	Delayed
Chlorambucil	$C_{14}H_{19}C_{l2}NO_2$	Slightly delayed	Delayed
Chlorhexidine	$C_{22}H_{30}C_{l2}N_{10}$	Non-effect	Toxic lethal
Ciclopirox ethanolamine	$C_{14}H_{24}N_2O_3$	Delayed	Severe delayed
Cinoxacin	$C_{12}H_{10}N_2O_5$	Delayed	Severe delayed
Clofibrate	$C_{12}H_{15}ClO_3$	Non-effect	Severe delayed
Clopidogrel	$C_{16}H_{16}ClNO_2S$	Non-effect	Delayed
Clorgyline hydrochloride	$C_{13}H_{16}Cl_3NO$	Delayed	Delayed
Colchicine	$C_{22}H_{25}NO_6$	Non-effect	Delayed
Deptropine citrate	$C_{29}H_{35}NO_8$	Delayed	Delayed
Desipramine hydrochloride	$C_{18}H_{23}ClN_2$	Delayed	Delayed
Diclofenac sodium	$C_{14}H_{10}Cl_2NNaO_2$	Delayed	Severe delayed
Dicumarol	$C_{19}H_{12}O_6$	Delayed	Severe delayed
Diethylstilbestrol	$C_{18}H_{20}O_2$	Delayed	Toxic lethal
Dimaprit dihydrochloride	$C_6H_{17}Cl_2N_3S$	Slightly delayed	Delayed
Disulfiram	$C_{10}H_{20}N_2S_4$	Delayed	Delayed
Dopamine hydrochloride	$C_8H_{12}ClNO_2$	Delayed	Delayed

Table 2 continued on next page

Table 2 continued

Chemical name	Chemical formula	Effect of 10 **μM**	Effect of 50 **μM**
Eburnamonine (-)	$C_{19}H_{22}N_2O$	Delayed	Delayed
Ethaverine hydrochloride	$C_{24}H_{30}ClNO_4$	Delayed	Delayed
Ethinylestradiol	$C_{20}H_{24}O_2$	Delayed	Severe delayed
Ethopropazine hydrochloride	$C_{19}H_{25}ClN_2S$	Delayed	Delayed
Ethoxyquin	$C_{14}H_{19}NO$	Non-effect	Delayed
Exemestane	$C_{20}H_{24}O_2$	Slightly delayed	Delayed
Ezetimibe	$C_{24}H_{21}F_2NO_3$	Slightly delayed	Delayed
Fenbendazole	$C_{15}H_{13}N_3O_2S$	Non-effect	Delayed
Fenoprofen calcium salt dihydrate	$C_{30}H_{30}CaO_8$	Slightly delayed	Delayed
Fentiazac	$C_{17}H_{12}ClNO_2S$	Toxic lethal	Toxic lethal
Floxuridine	$C_9H_{11}FN_2O_5$	Delayed	Toxic lethal
Flunixin meglumine	$C_{21}H_{28}F_3N_3O_7$	Delayed	Toxic lethal
Flutamide	$C_{11}H_{11}F_3N_2O_3$	Delayed	Toxic lethal
Fluticasone propionate	$C_{25}H_{31}F_3O_5S$	Non-effect	Delayed
Furosemide	$C_{12}H_{11}ClN_2O_5S$	Delayed	Delayed
Gatifloxacin	$C_{19}H_{22}FN_3O_4$	Delayed	Delayed
Gemcitabine	$C_9H_{11}F_2N_3O_4$	Delayed	Delayed
Gemfibrozil	$C_{15}H_{22}O_3$	Delayed	Toxic lethal
Gestrinone	$C_{21}H_{24}O_2$	Delayed	Delayed
Haloprogin	$C_9H_4Cl_3IO$	Delayed	Toxic lethal
Hexachlorophene	$C_{13}H_6Cl_6O_2$	Delayed	Severe delayed
Hexestrol	$C_{18}H_{22}O_2$	Slightly delayed	Delayed
Ibudilast	$C_{14}H_{18}N_2O$	Non-effect	Delayed
Idazoxan hydrochloride	$C_{11}H_{13}ClN_2O_2$	Slightly delayed	Delayed
Idazoxan hydrochloride	$C_{11}H_{13}ClN_2O_2$	Non-effect	Delayed
Idebenone	$C_{19}H_{30}O_5$	Severe delayed	Toxic lethal
Indomethacin	$C_{19}H_{16}ClNO_4$	Non-effect	Delayed
Ipriflavone	$C_{18}H_{16}O_3$	Delayed	Severe delayed
Isotretinoin	$C_{20}H_{28}O_2$	Non-effect	Severe delayed
Isradipine	$C_{19}H_{21}N_3O_5$	Non-effect	Delayed
Lansoprazole	$C_{16}H_{14}F_3N_3O_2S$	Slightly delayed	Delayed
Latanoprost	$C_{26}H_{40}O_5$	Non-effect	Delayed
Leflunomide	$C_{12}H_9F_3N_2O_2$	Delayed	Severe delayed
Letrozole	$C_{17}H_{11}N_5$	Non-effect	Delayed
Lithocholic acid	$C_{24}H_{40}O_3$	Non-effect	Delayed
Lodoxamide	$C_{11}H_6ClN_3O_6$	Non-effect	Delayed
Lofepramine	$C_{26}H_{27}ClN_2O$	Non-effect	Delayed
Loratadine	$C_{22}H_{23}ClN_2O_2$	Delayed	Delayed
Loxapine succinate	$C_{22}H_{24}ClN_3O_5$	Delayed	Delayed

Table 2 continued on next page

Table 2 continued

Chemical name	Chemical formula	Effect of 10 **μM**	Effect of 50 **μM**
Mebendazole	$C_{16}H_{13}N_3O_3$	Severe delayed	Severe delayed
Mebendazole	$C_{22}H_{26}N_2O_2$	Non-effect	Delayed
Meloxicam	$C_{14}H_{13}N_3O_4S_2$	Delayed	Toxic lethal
Methiazole	$C_{12}H_{15}N_3O_2S$	Delayed	Delayed
Mevastatin	$C_{23}H_{34}O_5$	Non-effect	Delayed
MK 801 hydrogen maleate	$C_{20}H_{19}NO_4$	Slightly delayed	Delayed
Nabumetone	$C_{15}H_{16}O_2$	Non-effect	Severe delayed
Naftopidil dihydrochloride	$C_{24}H_{30}Cl_2N_2O_3$	Slightly delayed	Delayed
Nandrolone	$C_{18}H_{26}O_2$	Delayed	Delayed
Naproxen sodium salt	$C_{14}H_{13}NaO_3$	Delayed	Delayed
Niclosamide	$C_{13}H_8Cl_2N_2O_4$	Delayed	Delayed
Nifekalant	$C_{19}H_{27}N_5O_5$	Delayed	Delayed
Niflumic acid	$C_{13}H_9F_3N_2O_2$	Delayed	Delayed
Nimesulide	$C_{13}H_{12}N_2O_5S$	Non-effect	Delayed
Nisoldipine	$C_{20}H_{24}N_2O_6$	Delayed	Toxic lethal
Nitazoxanide	$C_{12}H_9N_3O_5S$	Severe delayed	Severe delayed
Norethindrone	$C_{20}H_{26}O_2$	Non-effect	Delayed
Norgestimate	$C_{23}H_{31}NO_3$	Slightly delayed	Delayed
Oxfendazol	$C_{15}H_{13}N_3O_3S$	Slightly delayed	Delayed
Oxibendazol	$C_{12}H_{15}N_3O_3$	Severe delayed	Severe delayed
Oxymetholone	$C_{21}H_{32}O_3$	Slightly delayed	Delayed
Parbendazole	$C_{13}H_{17}N_3O_2$	Severe delayed	Severe delayed
Parthenolide	$C_{15}H_{20}O_3$	Non-effect	Delayed
Penciclovir	$C_{10}H_{15}N_5O_3$	Non-effect	Delayed
Pentobarbital	$C_{11}H_{18}N_2O_3$	Non-effect	Delayed
Phenazopyridine hydrochloride	$C_{11}H_{12}ClN_5$	Delayed	Toxic lethal
Phenothiazine	$C_{12}H_9NS$	Non-effect	Delayed
Phenoxybenzamine hydrochloride	$C_{18}H_{23}Cl_2NO$	Non-effect	Delayed
Pizotifen malate	$C_{23}H_{27}NO_5S$	Delayed	Severe delayed
Pramoxine hydrochloride	$C_{17}H_{28}ClNO_3$	Slightly delayed	Delayed
Prilocaine hydrochloride	$C_{13}H_{21}ClN_2O$	Non-effect	Delayed
Primidone	$C_{12}H_{14}N_2O_2$	Slightly delayed	Delayed
Racecadotril	$C_{21}H_{23}NO_4S$	Slightly delayed	Delayed
Riluzole hydrochloride	$C_8H_6ClF_3N_2OS$	Non-effect	Delayed
Ritonavir	$C_{37}H_{48}N_6O_5S_2$	Non-effect	Severe delayed
S(-)Eticlopride hydrochloride	$C_{17}H_{26}Cl_2N_2O_3$	Delayed	Delayed
Salmeterol	$C_{25}H_{37}NO_4$	Non-effect	Delayed
Streptomycin sulfate	$C_{42}H_{84}N_{14}O_{36}S_3$	Non-effect	Delayed
Sulconazole nitrate	$C_{18}H_{16}Cl_3N_3O_3S$	Delayed	Delayed

Table 2 continued on next page

Table 2 continued

Chemical name	Chemical formula	Effect of 10 **μM**	Effect of 50 **μM**
Tegafur	$C_8H_9FN_2O_3$	Delayed	Delayed
Telmisartan	$C_{33}H_{30}N_4O_2$	Severe delayed	Toxic lethal
Tenatoprazole	$C_{16}H_{18}N_4O_3S$	Non-effect	Delayed
Terbinafine	$C_{21}H_{25}N$	Non-effect	Delayed
Thimerosal	$C_9H_9HgNaO_2S$	Non-effect	Delayed
Thiorphan	$C_{12}H_{15}NO_3S$	Delayed	Delayed
Tolcapone	$C_{14}H_{11}NO_5$	Severe delayed	Severe delayed
Topotecan	$C_{23}H_{23}N_3O_5$	Delayed	Delayed
Tracazolate hydrochloride	$C_{16}H_{25}ClN_4O_2$	Severe delayed	Delayed
Tribenoside	$C_{29}H_{34}O_6$	Delayed	Delayed
Triclabendazole	$C_{14}H_9Cl_3N_2OS$	Delayed	Delayed
Triclosan	$C_{12}H_7Cl_3O_2$	Delayed	Severe delayed
Trioxsalen	$C_{14}H_{12}O_3$	Delayed	Delayed
Troglitazone	$C_{24}H_{27}NO_5S$	Severe delayed	Toxic lethal
Valproic acid	$C_8H_{16}O_2$	Non-effect	Delayed
Voriconazole	$C_{16}H_{14}F_3N_5O$	Non-effect	Delayed
Zardaverine	$C_{12}H_{10}F_2N_2O_3$	Slightly delayed	Delayed
Zuclopenthixol dihydrochloride	$C_{22}H_{27}Cl_3N_2OS$	Delayed	Delayed

metastatic cancer cells (***Liu et al., 2013***). This evidence suggests that epiboly-interrupting drugs have the potential for suppressing metastasis of human cancer cells.

Identified drugs suppressed cell motility and invasion of human cancer cells

It has been reported that zebrafish have orthologues to 86% of 1318 human drug targets (***Gunnarsson et al., 2008***). However, it was not known whether the epiboly-interrupting drugs could suppress metastatic dissemination of human cancer cells. To test this, we subjected the 78 epiboly-interrupting drugs that showed a suppressor effect on epiboly progression at a 10 μM concentration to in vitro experiments using a human cancer cell line. The experiments examined whether the drugs could suppress cell motility and invasion of MDA-MB-231 cells through a Boyden chamber. Before conducting the experiment, we investigated whether these drugs might affect viability of MDA-MB-231 cells using an MTT assay. Out of the 78 drugs, 16 of them strongly affected cell viability at concentrations less than 1 μM and were not used in the cell motility experiments. The remaining 62 drugs were assayed in Boyden chamber motility experiments. Out of the 62 drugs, 20 of the drugs inhibited cell motility and invasion of MDA-MB-231 cells without affecting cell viability. Among the 20 drugs, hexachlorophene and nitazoxanide were removed since the primary targets of the drugs, D-lactate dehydrogenase and pyruvate ferredoxin oxidoreductase, are not expressed in mammalian cells. With the exception of ipriflavone, whose target is still unclear, the known primary targets of the remaining 17 drugs are reported to be expressed by mammalian cells (***Figure 2A*** and ***Table 3***).

We confirmed that highly metastatic human cancer cell lines expressed target genes through western blotting analyses. Among the genes, serotonin receptor 2C (HTR2C), which is a primary target of pizotifen, was highly expressed in only metastatic cell lines (***Figure 2B*** and ***Figure 2—figure supplement 2A***). Clinical data also shows that that HTR2C expression is correlated with tumor stage of breast cancer patients and is higher in metastatic and Her2/neu-overexpressing tumors (***Pai et al., 2009***). Pizotifen suppressed cell motility and invasion of several highly metastatic human cancer cell lines in a dose-dependent manner (***Figure 2C***). Similarly, dopamine receptor D2 (DRD2), which is a

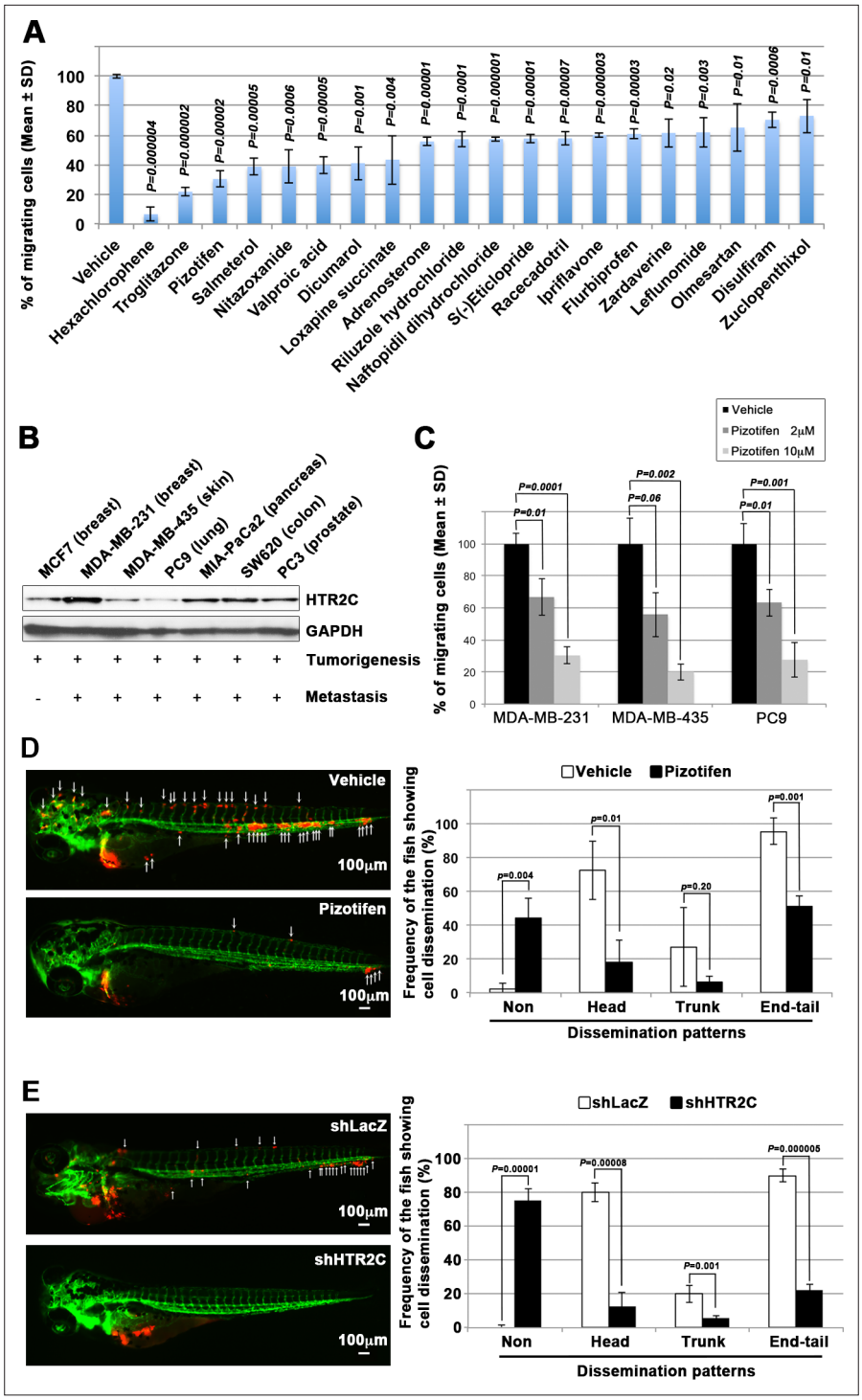

Figure 2. Pizotifen, one of epiboly-interrupting drugs, suppressed metastatic dissemination of human cancer cells lines in vivo and vitro. (**A**) Effect of the epiboly-interrupting drugs on cell motility and invasion of MBA-MB-231 cells. MBA-MB-231 cells were treated with vehicle or each of the epiboly-interrupting drugs and then subjected to Boyden chamber assays. Fetal bovine serum (1% v/v) was used as the chemoattractant in both assays. Each experiment was performed at least twice. (**B**) Western blot analysis of HTR2C levels (top) in a non-metastatic human cancer cell line, MCF7 (breast) and highly metastatic human cancer cell lines, MDA-MB-231 (breast), MDA-MB-435 (melanoma), PC9 (lung), MIA-PaCa2 (pancreas), PC3 (prostate), and SW620 (colon); GAPDH loading control is shown (bottom). (**C**) Effect of pizotifen on cell motility and invasion of MBA-MB-231, MDA-MB-435, and PC9 cells. Either vehicle or pizotifen treated the cells were subjected to Boyden chamber assays. Fetal bovine

Figure 2 continued on next page

Figure 2 continued

serum (1% v/v) was used as the chemoattractant in both assays. Each experiment was performed at least twice. (**D**) and (**E**) Representative images of dissemination of 231R, shLacZ 231R or shHTR2C 231R cells in zebrafish xenotransplantation model. The fish larvae that were inoculated with 231R cells were treated with either vehicle (top left) or the drug (lower left) (**D**). The fish larvae that were inoculated with either shLacZ 231R or shHTR2C 231R cells (lower left) (**E**). White arrows head indicate disseminated 231R cells. The images were shown in 4× magnification. Scale bar, 100 μm. The mean frequencies of the fish showing head, trunk, or end-tail dissemination were counted (graph on right). Each value is indicated as the mean ± SEM of two independent experiments. Statistical analysis was determined by Student's t test.

The online version of this article includes the following figure supplement(s) for figure 2:

Figure supplement 1. Blocking Dopamine receptor D2 with S(-) Eticlopride hydrochloride suppressed cell motility and invasion of highly metastatic human cancer cells in a dose-dependent manner.

Figure supplement 2. Pizotifen suppressed metastatic dissemination of MDA-MB-231 and MIA-PaCa2 cells in a zebrafish xenotransplantation model.

primary target of S(-)eticlopride hydrochloride, was highly expressed in only metastatic cell lines, and the drug suppressed cell motility and invasion of these cells in a dose-dependent manner (***Figure 2—figure supplement 2A-C***).

These results indicate that a number of the epiboly-interrupting drugs also have suppressor effects on cell motility and invasion of highly metastatic human cancer cells.

Table 3. Primary targets of the identified drugs.

The identified drugs	Primary targets of the identified drugs
Hexachlorophene	D-Lactate dehydrogenase (D-LDH), not expressed in mammalian cells
Troglitazone	Agonist for peroxisome proliferator-activated receptor α and γ (PPARα and -γ)
Pizotifen malate	5-Hydroxytryptamine receptor 2C (HTR2C)
Salmeterol	Adrenergic receptor beta 2 (ADRB2)
Nitazoxanide	Pyruvate ferredoxin oxidoreductase (PFOR), not expressed in mammalian cells
Valproic acid	Histone deacetylases (HDACs)
Dicumarol	NAD(P)H dehydrogenase quinone 1 (NQO1)
Loxapine succinate	Dopamine receptor D2 and D4 (DRD2 and DRD4)
Adrenosterone	Hydroxysteroid (11-beta) dehydrogenase 1 (HSD11β1)
Riluzole hydrochloride	Glutamate R and voltage-dependent Na+ channel
Naftopidil dihydrochloride	5-Hydroxytryptamine receptor 1A (HTR1A) and α1-adrenergic receptor (AR)
S(-)Eticlopride hydrochloride	Dopamine receptor D2 (DRD2)
Racecadotril	Membrane metallo-endopeptidase (MME)
Ipriflavone	Unknown
Flurbiprofen	Cyclooxygenase 1 and 2 (Cox1 and -2)
Zardaverine	Phosphodiesterase III/IV (PDE3/4)
Leflunomide	Dihydroorotate dehydrogenase (DHODH)
Olmesartan	Angiotensin II receptor alpha
Disulfiram	Aldehyde dehydrogenase (ALDH) Dopamine β-hydroxylase (DBH)
Zuclopenthixol dihydrochloride	Dopamine receptors D1 and D2 (DRD1 and -2)

Pizotifen suppressed metastatic dissemination of human cancer cells in a zebrafish xenotransplantation model

While a number of the epiboly-interrupting drugs suppressed cell motility and invasion of human cell lines in vitro, it was still unclear whether the drugs could suppress metastatic dissemination of cancer cells in vivo. Therefore, we examined whether the identified drugs could suppress metastatic dissemination of these human cancer cells in a zebrafish xenotransplantation model. Pizotifen was selected to test since HTR2C was overexpressed only in highly metastatic cell lines supporting the hypothesis that it could be a novel target for blocking metastatic dissemination of cancer cells (***Figure 2B***). Red fluorescent protein (RFP)-labelled MDA-MB-231 (231R) cells were injected into the duct of Cuvier of *Tg (kdrl:eGFP)* zebrafish at 2 dpf and then maintained in the presence of either vehicle or pizotifen. Twenty-four hours post injection, the numbers of fish showing metastatic dissemination of 231R cells were measured via fluorescence microscopy. In this model, the dissemination patterns were generally divided into three categories: (i) head dissemination, in which disseminated 231R cells exist in the vessel of the head part; (ii) trunk dissemination, in which the cells were observed in the vessel dilating from the trunk to the tail; (iii) end-tail dissemination, in which the cells were observed in the vessel of the end-tail part (***Nakayama et al., 2020***).

Three independent experiments revealed that the frequencies of fish in the drug-treated group showing head, trunk, or end-tail dissemination significantly decreased to 55.3% ± 7.5%, 28.5 ± 5.0%, or 43.5% ± 19.1% when compared with those in the vehicle-treated group; 95.8% ± 5.8%, 47.1 ± 7.7%, or 82.6% ± 12.7%. Conversely, the frequency of the fish in the drug-treated group not showing any dissemination significantly increased to 45.4% ± 0.5% when compared with those in the vehicle-treated group; 2.0% ± 2.9% (***Figure 2D***, ***Figure 2—figure supplement 2*** and ***Table 4***).

Similar effects were observed in another xenograft experiments using an RFP-labelled human pancreatic cancer cell line, MIA-PaCa-2 (MP2R). In the drug-treated group, the frequencies of the fish showing head, trunk, or end-tail dissemination significantly decreased to 15.3% ± 6.7%, 6.2% ± 1.3%, or 41.1% ± 1.5%; conversely, the frequency of the fish not showing any dissemination significantly increased to 46.3% ± 8.9% when compared with those in the vehicle-treated group; 74.5% ± 11.1%, 18.9% ± 14.9%, 77.0% ± 9.0%, or 17.2% ± 0.7% (***Figure 2—figure supplement 2A*** and ***Table 5***).

To eliminate the possibility that the metastasis suppressing effects of pizotifen might result from off-target effects of the drug, we conducted validation experiments to determine whether knockdown of HTR2C would show the same effects. Sub-clones of 231R cells that expressed short hairpin RNA (shRNA) targeting either LacZ or HTR2C were injected into the fish at 2 dpf and the fish were maintained in the absence of drug. In the fish that were inoculated with shHTR2C 231R cells, the frequencies of the fish showing head, trunk, and end-tail dissemination significantly decreased to 6.7% ± 4.9%, 6.7% ± 0.7%, or 20.0% ± 16.5%; conversely, the frequency of the fish not showing any dissemination significantly increased to 80.0% ± 4.4% when compared with those that were inoculated with shLacZ 231R cells; 80.0% ± 27.1%, 20.0% ± 4.5%, 90.0% ± 7.7%, or 0% (***Figure 2E*** and ***Table 6***).

These results indicate that pharmacological and genetic inhibition of HTR2C suppressed metastatic dissemination of human cancer cells in vivo.

Pizotifen suppressed metastasis progression of a mouse model of metastasis

We examined the metastasis-suppressor effect of pizotifen in a mouse model of metastasis (***Tao et al., 2008***). Luciferase-expressing 4T1 murine mammary carcinoma cells were inoculated into the mammary fat pads (MFP) of female BALB/c mice. On day 2 post inoculation, the mice were randomly assigned to two groups and one group received once daily intraperitoneal injections of 10 mg/kg pizotifen while the other group received a vehicle injection. Bioluminescence imaging and tumor measurement revealed that the sizes of the primary tumors in pizotifen-treated mice were equal to those in the vehicle-treated mice on day 10 post inoculation. The primary tumors were resected after the analyses. Immunofluorescence (IF) staining also demonstrated that the percentage of Ki67-positive cells in the resected primary tumors of pizotifen-treated mice were the same as those of vehicle-treated mice (***Figure 3A–C***), additionally, both groups showed less than 1% cleaved caspase 3 positive cells (***Figure 3—figure supplement 1***). Therefore, no anti-tumor effect of pizotifen was observed on the primary tumor. After 70 days from inoculation, bioluminescence imaging detected light emitted in the lungs, livers, and lymph nodes of vehicle-treated mice but not those of pizotifen-treated mice

Table 4. Effects of pharmacological inhibition of HTR2C on metastatic dissemination of MDA-MB-231 cells in zebrafish xenografted models.
Related to ***Figure 2D***. The numbers and frequencies of the fish showing the dissemination patterns in vehicle- or pizotifen-treated group were indicated. The fish showed both patterns of dissemination were redundantly counted in this analysis.

		Experiment _#1	Experiment _#2	Experiment _#3	Average of experiments
Drug: Vehicle Cell: MDA-MB-231	Non-dissemination	0% n1 = 0/17	0% n2 = 0/12	6.66% n3 = 1/15	2.22% ± 3.84%
	Head	58.82% n1 = 10/17	91.66% n2 = 11/12	6.66% n3 = 1/15	72.38% ± 17.15%
	Trunk	52.94% n1 = 9/17	8.33% n2 = 1/12	20% n3 = 2/15	27.09% ± 23.13%
	End-tail	100% n1 = 17/17	100% n2 = 12/12	86.66% n3 = 13/15	95.55% ± 7.69%
Drug: Pizotifen Cell: MDA-MB-231	Non-dissemination	55% n1 = 11/20	31.57% n2 = 6/19	45.45 % n3 = 10/22	44.01% ± 11.77%
	Head	5% n1 = 1/20	31.57% n2 = 6/19	18.18% n3 = 4/22	18.25% ± 13.28%
	Trunk	5% n1 = 1/20	10.52% n2 = 2/19	4.45% n3 = 1/22	6.69% ± 3.32%
	End-tail	45% n1 = 9/20	57.89% n2 = 11/19	50% n3 = 11/22	50.96% ± 6.50%

Table 5. Effects of pharmacological inhibition of HTR2C on metastatic dissemination of Mia-PaCa2 cells in zebrafish xenografted models.

Related to ***Figure 4***. The numbers and frequencies of the fish showing the dissemination patterns in vehicle- or pizotifen-treated group were indicated. The fish showed both patterns of dissemination were redundantly counted in this analysis.

		Experiment _#1	Experiment _#2	Average of experiments
Drug: Vehicle Cell: MIA-PaCa2	Non-dissemination	17.64% n1 = 3/17	16.66% n2 = 2/12	17.15% + 0.69%
	Head	82.35% n1 = 14/17	66.66% n2 = 8/12	74.50% + 11.09%
	Trunk	29.41% n1 = 5/17	8.33% n2 = 1/12	18.87% + 14.90%
	End-tail	70.58% n1 = 12/17	83.33% n2 = 10/17	76.96% + 9.01
Drug: Pizotifen Cell: MIA-PaCa2	Non-dissemination	40% n1 = 4/10	52.63% n2 = 10/19	46.31% + 8.93%
	Head	20% n1 = 2/10	10.52% n2 = 2/19	15.26% + 6.69%
	Trunk	10% n1 = 1/10	5.26% n2 = 1/19	7.63% + 3.34%
	End-tail	40% n1 = 4/10	42.05% n2 = 8/19	41.4% + 1.48%

(***Figure 3C***). Vehicle-treated mice formed 5–50 metastatic nodules per lung in all 10 mice analyzed; conversely, pizotifen-treated mice (n = 10) formed 0–5 nodules per lung in all 10 mice analyzed (***Figure 3D***). Histological analyses confirmed that metastatic lesions in the lungs were detected in all vehicle-treated mice; conversely, they were detected in only 2 of 10 pizotifen-treated mice and the rest of the mice showed metastatic colony formations around the bronchiole of the lung. In addition, 4 of 10 vehicle-treated mice exhibited metastasis in the liver and the rest showed metastatic colony formation around the portal tract of the liver. In contrast, none of 10 pizotifen-treated mice showed liver metastases and only half of the 10 mice showed metastatic colony formation around the portal tract (***Figure 3E***). These results indicate that pizotifen can suppress metastasis progression without affecting primary tumor growth.

To eliminate the possibility that the metastasis suppressing effects of pizotifen might result from off-target effects, we conducted validation experiments to determine whether knockdown of HTR2C would show the same effects. The basic experimental process followed the experimental design described above except that sub-clones of 4T1 cells that expressed shRNA targeting either LacZ or HTR2C were injected into the MFP of female BALB/c mice and the mice were maintained without

Table 6. Effects of genetic inhibition of HTR2C on metastatic dissemination of MDA-MB-231 cells in zebrafish xenografted models.

Related to ***Figure 2E***. The numbers and frequencies of the fish showing the dissemination patterns in the zebrafish that were inoculated with either shLacZ or shHTR2C MDA-MB-231 cells were indicated. The fish showed both patterns of dissemination were redundantly counted in this analysis.

		Experiment _#1	Experiment _#2	Average of experiments
shLacZ	Non-dissemination	0% n1 = 0/10	0% n2 = 0/10	0%
	Head	60% n1 = 6/10	100% n2 = 10/10	80% ± 28.28%
	Trunk	30% n1 = 3/10	10% n2 = 1/10	20% ± 14.14%
	End-tail	80% n1 = 8/10	100% n2 = 10/10	90% ± 14.14
shHTR2C	Non-dissemination	80% n1 = 12/15	76.84% n2 = 14/19	76.84 ± 4.46 %
	Head	6.66% n1 = 1/15	15.78% n2 = 3/19	11.22% ± 6.45%
	Trunk	6.66% n1 = 1/15	5.26% n2 = 1/19	5.96% ± 0.99%
	End-tail	20% n1 = 3/15	26.31% n2 = 5/19	23.15% ± 4.46%

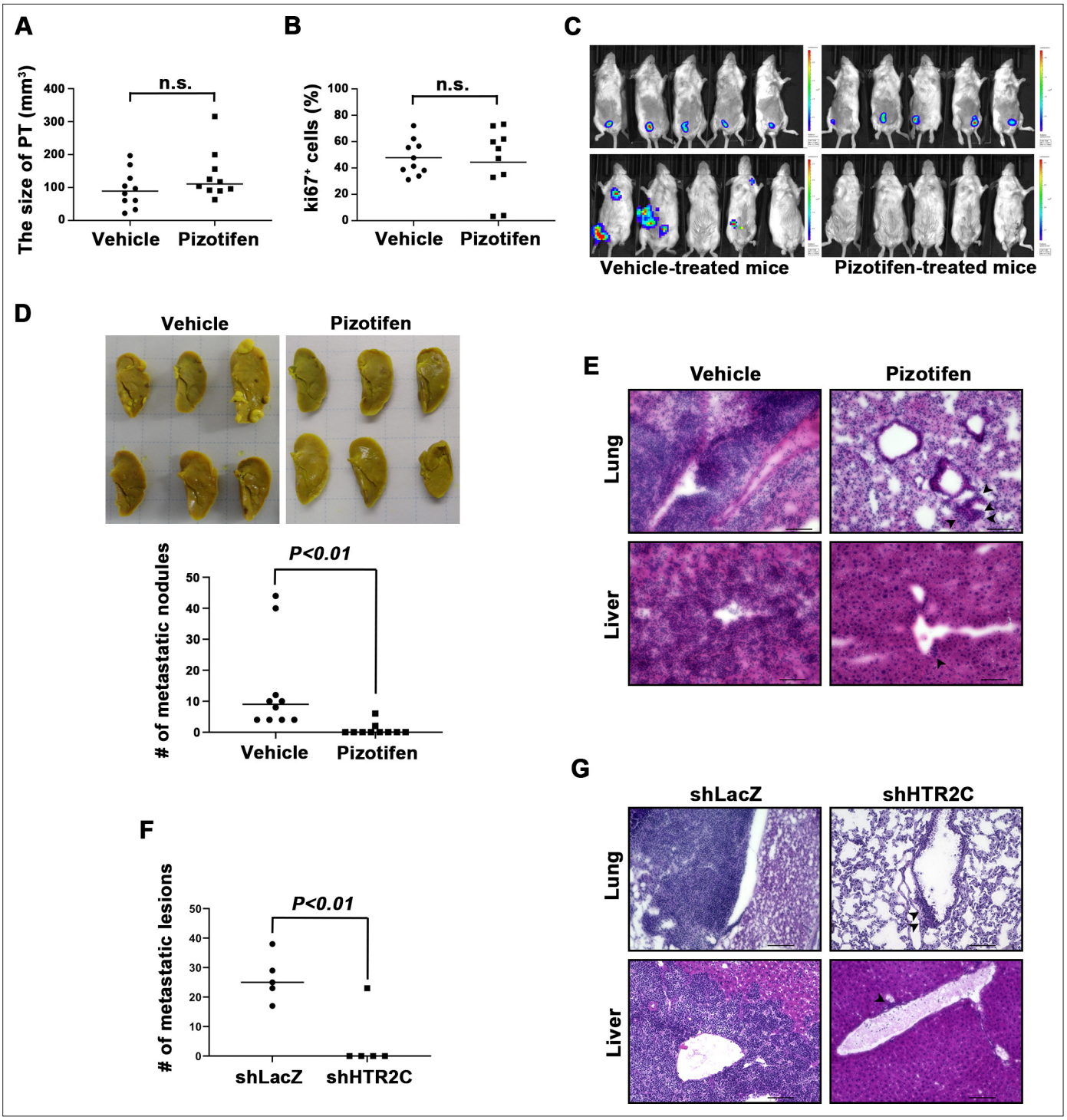

Figure 3. Pizotifen suppressed metastatic progression in a mouse model of metastasis. (**A**) Mean volumes (n = 10 per group) of 4T1 primary tumors formed in the mammary fat pad of either vehicle- or pizotifen-treated mice at day 10 post injection. (**B**) Ki67 expression level in 4T1 primary tumors formed in the mammary fat pad of either vehicle- or pizotifen-treated mice at day 10 post injection. The mean expression levels of Ki67 (n = 10 mice per group) were determined and were calculated as the mean ration of Ki67-positive cells to 4′,6-diamidino-2-phenylindole (DAPI) area. (**C**) Representative images of primary tumors on day 10 post injection (top panels) and metastatic burden on day 70 post injection (bottom panels) taken using an IVIS Imaging System. (**D**) Representative images of the lungs from either vehicle- (top) or pizotifen-treated mice (bottom) at 70 days post tumor inoculation. Number of metastatic nodules in the lung of either vehicle- or pizotifen-treated mice (right). (**E**) Representative hematoxylin and eosin (H&E) staining of the lung (top) and liver (bottom) from either vehicle- or pizotifen-treated mice. Black arrow heads indicate metastatic 4T1 cells. (**F**) The mean number of metastatic lesions in step sections of the lungs from the mice that were inoculated with 4T1-12B cells expressing short hairpin RNA (shRNA) targeting

Figure 3 continued on next page

Figure 3 continued

for either LacZ or HTR2C. (**G**) Representative H&E staining of the lung and liver from the mice that were inoculated with 4T1-12B cells expressing shRNA targeting for either LacZ or HTR2C. Black arrow heads indicate metastatic 4T1 cells. Each value is indicated as the mean ± SEM. Statistical analysis was determined by Student's t test.

The online version of this article includes the following figure supplement(s) for figure 3:

Figure supplement 1. Cleaved caspase 3 expression level in 4T1 primary tumors formed in the mammary fat pad of either vehicle- or pizotifen-treated mice at day 10 post injection.

drug. Histological analyses revealed that all of the mice (n = 5) that were inoculated with 4T1 cells expressing shRNA targeting LacZ showed metastases in the lungs. The mean number of metastatic lesions in a lung was 26.4 ± 7.8. In contrast, only one of the mice (n = 5) were inoculated with 4T1 cells expressing shRNA targeting HTR2C showed metastases in the lungs and the rest of the mice showed metastatic colony formation around the bronchiole of the lung. The mean number of metastatic lesions in the lung significantly decreased to 10% of those of mice that were inoculated with 4T1 cells expressing shRNA targeting LacZ (***Figure 3F–H***).

Taken together, pharmacological and genetic inhibition of HTR2C showed an anti-metastatic effect in the 4T1 model system.

HTR2C promoted EMT-mediated metastatic dissemination of human cancer cells

Although pharmacological and genetic inhibition of HTR2C inhibited metastasis progression, a role for HTR2C on metastatic progression has not been reported. Therefore, we examined whether HTR2C could confer metastatic properties on poorly metastatic cells.

First, we established a stable sub-clone of MCF7 human breast cancer cells expressing either vector control or HTR2C. Vector control expressing MCF7 cells maintained highly organized cell-cell adhesion and cell polarity; however, HTR2C-expressing MCF7 cells led to loss of cell-cell contact and cell scattering. The cobblestone-like appearance of these cells was replaced by a spindle-like, fibroblastic morphology. Western blotting and IF analyses revealed that HTR2C-expressing MCF7 cells showed loss of E-cadherin and EpCAM, and elevated expressions of N-cadherin, vimentin, and an EMT-inducible transcriptional factor ZEB1. Similar effects were validated through another experiment using an immortal keratinocyte cell line, HaCaT cells, in that HTR2C-expressing HaCaT cells also showed loss of cell-cell contact and cell scattering with loss of epithelial markers and gain of mesenchymal markers (***Figure 4A–C*** and ***Figure 4—figure supplement 1A***). Therefore, both the morphological and molecular changes in the HTR2C-expressing MCF7 and HaCaT cells demonstrated that these cells had undergone an EMT.

Next, we examined whether HTR2C-driven EMT could promote metastatic dissemination of human cancer cells. Boyden chamber assay revealed that HTR2C expressing MCF7 cells showed an increased cell motility and invasion compared with vector control-expressing MCF7 cells in vitro (***Figure 4D***). Moreover, we conducted in vivo examination of whether HTR2C expression could promote metastatic dissemination of human cancer cells in a zebrafish xenotransplantation model. RFP-labelled MCF7 cells expressing either vector control or HTR2C were injected into the duct of Cuvier of *Tg* (*kdrl:eGFP*) zebrafish at 2 dpf. Twenty-four hours post injection, the frequencies of the fish showing metastatic dissemination of the inoculated cells were measured using fluorescence microscopy. In the fish that were inoculated with HTR2C expressing MCF7 cells, the frequencies of the fish showing head, trunk, and end-tail dissemination significantly increased to 96.7% ± 4.7%, 68.8% ± 6.4%, or 89.5% ± 3.4%; conversely, the frequency of the fish not showing any dissemination decreased to 0% when compared with those in the fish that were inoculated with vector control expressing MCF7 cells; 33.1% ± 18.5%, 0%, 56.9% ± 4.4%, or 43% (***Figure 4E***, ***Figure 4—figure supplement 1B*** and ***Table 7***).

These results indicated that HTR2C promoted metastatic dissemination of cancer cells through induction of EMT, and suggest that the screen can easily be converted to a chemical genetic screening platform.

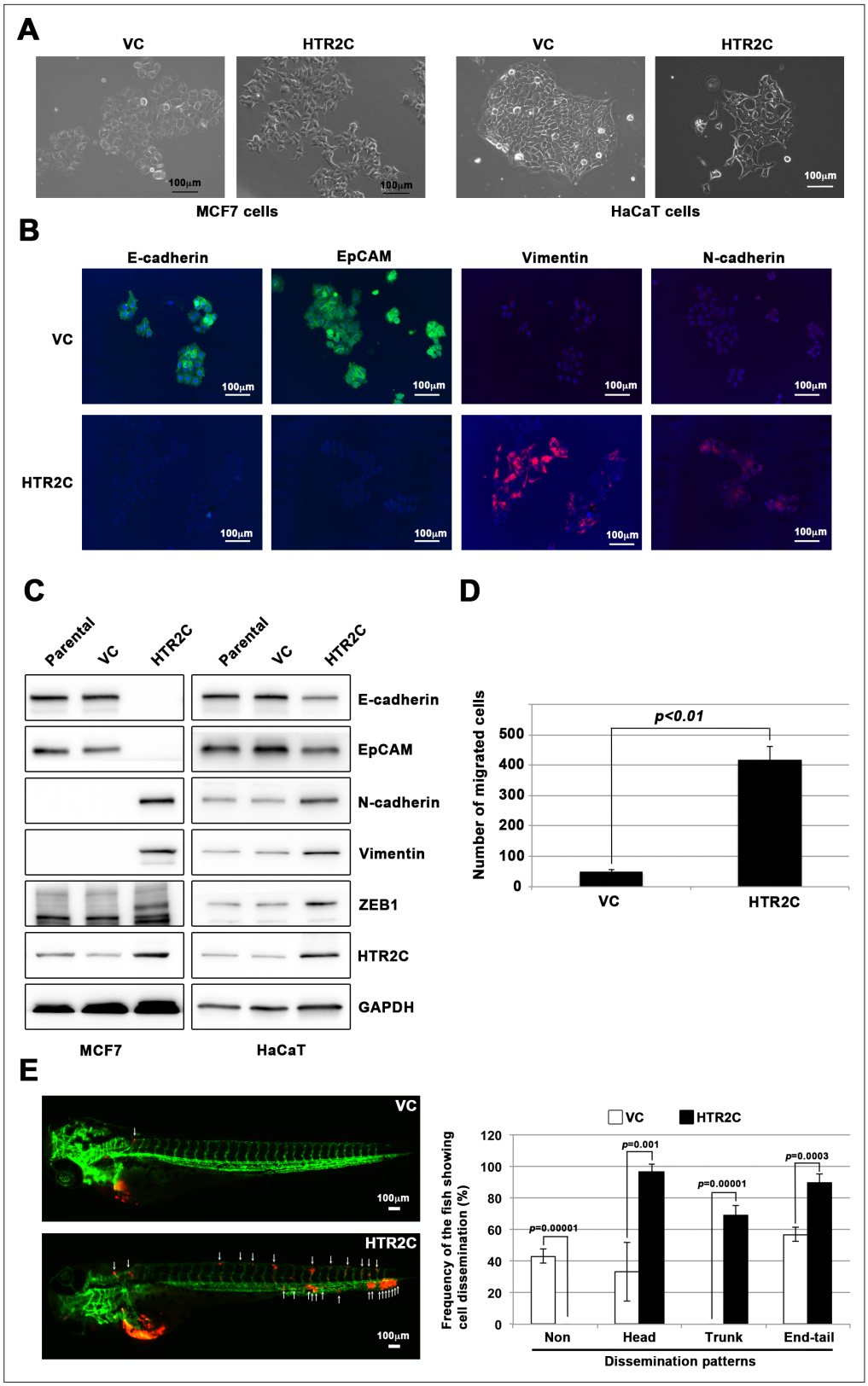

Figure 4. HTR2C induced epithelial-to-mesenchymal transition (EMT)-mediated metastatic dissemination of human cancer cells. (**A**) The morphologies of the MCF7 and HaCaT cells expressing either the control vector or HTR2C were revealed by phase contrast microscopy. (**B**) Immunofluorescence staining of E-cadherin, EpCAM, vimentin, and N-cadherin expressions in the MCF7 cells from A. (**C**) Expression of E-cadherin, EpCAM, vimentin,

Figure 4 continued on next page

Figure 4 continued

N-cadherin, and HTR2C was examined by western blotting in the MCF7 and HaCaT cells; GAPDH loading control is shown (bottom). (**D**) Effect of HTR2C on cell motility and invasion of MCF7 cells. MCF7 cells were subjected to Boyden chamber assays. Fetal bovine serum (1% v/v) was used as the chemoattractant in both assays. Each experiment was performed at least twice. (**E**) Representative images of dissemination patterns of MCF7 cells expressing either the control vector (top left) or HTR2C (lower left) in a zebrafish xenotransplantation model. White arrow heads indicate disseminated MCF7 cells. The mean frequencies of the fish showing head, trunk, or end-tail dissemination tabulated (right). Each value is indicated as the mean ± SEM of two independent experiments. Statistical analysis was determined by Student's t test.

The online version of this article includes the following figure supplement(s) for figure 4:

Figure supplement 1. HTR2C promoted EMT-mediated metastatic dissemination of poorly metastatic human cancer cells in a zebrafish xenotransplantation model.

Pizotifen induced mesenchymal-to-epithelial transition through inhibition of Wnt signaling

Finally, we elucidated the mechanism of action of how pizotifen suppressed metastasis, especially metastatic dissemination of cancer cells. Our results showed that HTR2C induced EMT and that pharmacological and genetic inhibition of HTR2C suppressed metastatic dissemination of MDA-MB-231 cells that had already transitioned to mesenchymal-like traits via EMT. Therefore, we speculated that blocking HTR2C with pizotifen might inhibit the molecular mechanisms which follow EMT induction. We first investigated the expressions of epithelial and mesenchymal markers in pizotifen-treated MDA-MB-231 cells since the activation of an EMT program needs to be transient and reversible, and transition from a fully mesenchymal phenotype to a epithelial-mesenchymal hybrid state or a fully epithelial phenotype is associated with malignant phenotypes (***Kröger et al., 2019***). IF and FACS analyses revealed 20% of pizotifen-treated MDA-MB-231 cells restored E-cadherin expression. Also, western blotting analysis demonstrated that 4T1 primary tumors from pizotifen-treated mice has elevated E-cadherin expression compared with tumors from vehicle-treated mice (***Figure 5A–C*** and ***Figure 5—figure supplement 1***). However, mesenchymal markers did not change between vehicle and pizotifen-treated MDA-MB-231 cells (data not shown). We further analyzed E-cadherin-positive (E-cad$^+$) cells in pizotifen-treated MDA-MB-231 cells. The E-cad$^+$ cells showed elevated expressions of epithelial markers KRT14 and KRT19; and decreased expression of mesenchymal makers vimentin, MMP1, MMP3, and S100A4. Recent research reports that an EMT program needs to be transient and reversible and that a mesenchymal phenotype in cancer cells is achieved by constitutive ectopic expression of ZEB1. In accordance with the research, the E-cad$^+$ cells and 4T1 primary tumors from

Table 7. Effects of HTR2C overexpression on metastatic dissemination of MCF7 cells in zebrafish xenografted models.

Related to ***Figure 4E***. The numbers and frequencies of the fish showing the dissemination patterns in the zebrafish that were inoculated with MCF7 cells expressing either vector control (VC) or HTR2C were indicated. The fish showed both patterns of dissemination were redundantly counted in this analysis.

		Experiment _#1	Experiment _#2	Average of experiments
VC	Non-dissemination	46.15% n1 = 6/13	40% n2 = 4/10	43.07% ± 4.35%
	Head	46.15% n1 = 6/13	20% n2 = 2/10	33.07% ± 18.49%
	Trunk	0% n1 = 0/13	0% n2 = 0/10	0%
	End-tail	53.84% n1 = 7/13	60% n2 = 6/10	56.92% ± 4.35%
HTR2C	Non-dissemination	0% n1 = 0/14	0% n2 = 0/15	0%
	Head	100% n1 = 14/14	93.33% n2 = 14/15	96.66% ± 4.71%
	Trunk	64.28% n1 = 9/14	73.33% n2 = 11/15	68.80% ± 6.39%
	End-tail	85.71% n1 = 12/14	93.33% n2 = 14/15	89.52% ± 5.38%

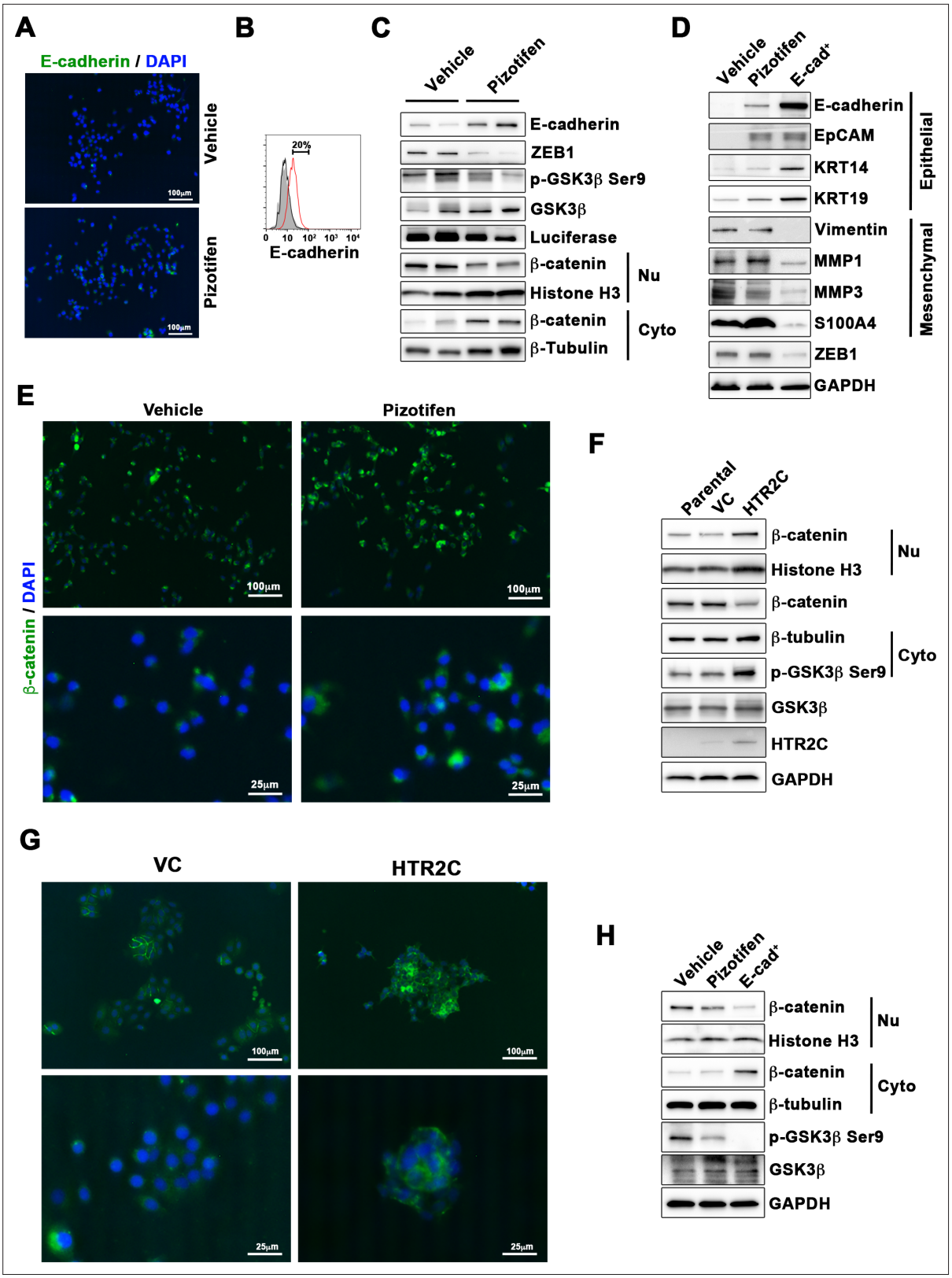

Figure 5. Pizotifen restored mesenchymal-like traits of MDA-MB-231 cells into epithelial traits through blocking nuclear accumulation of β-catenin. (**A**) Immunofluorescence (IF) staining of E-cadherin in either vehicle- or pizotifen-treated MDA-MB-231 cells. (**B**) Surface expression of E-cadherin in either vehicle (black)- or pizotifen (red)-treated MDA-MB-231 cells by FACS analysis. Non-stained controls are shown in gray. (**C**) Protein expressions levels of E-cadherin, ZEB1, and β-catenin in the cytoplasm and nucleus of 4T1 primary tumors from either vehicle- or pizotifen-treated mice are shown;

Figure 5 continued on next page

Figure 5 continued

Luciferase, histone H3, and β-tubulin are used as loading control for whole cell, nuclear, or cytoplasmic lysate, respectively. (**D**) Protein expression levels of epithelial and mesenchymal markers and ZEB1 in either vehicle- or pizotifen-treated MDA-MB-231 cells or E-cadherin-positive (E-cad$^+$) cells in pizotifen-treated MDA-MB-231 cells are shown. (**E**) IF staining of β-catenin in the MCF7 cells expressing either vector control (top left, bottom left) or HTR2C (top right, bottom right). (**F**) Expressions of β-catenin in the cytoplasm and nucleus of MCF7 cells. (**G**) IF staining of β-catenin in either vehicle (top left, bottom left) or pizotifen-treated MDA-MB-231 cells (top right, bottom right). (**H**) Expressions of β-catenin in the cytoplasm and nucleus of MDA-MB-231 cells and the E-cad$^+$ cells.

The online version of this article includes the following figure supplement(s) for figure 5:

Figure supplement 1. Quantification analyses of western blotting bands in ***Figure 5C***.

Figure supplement 2. Quantification analyses of western blotting bands in ***Figure 5D***.

Figure supplement 3. Quantification analyses of western blotting bands in ***Figure 5F***.

Figure supplement 4. Expression of Snail and Twist1 was examined by western blotting in the MCF7 cells (left); GAPDH loading control is shown (bottom).

Figure supplement 5. Quantification analyses of western blotting bands in ***Figure 5H***.

pizotifen-treated mice had decreased ZEB1 expression compared with vehicle-treated cells and tumors from vehicle-treated mice (***Figure 5D*** and ***Figure 5—figure supplement 2***). In contrast, HTR2C-expressing MCF7 and HuMEC cells expressed ZEB1 but not vehicle control MCF7 and HuMEC cells (***Figure 4C*** and ***Figure 5—figure supplement 3***). HTR2C-expressing MCF7 cells expressed not only ZEB1 but also Twist1 and Snail. In contrast, pizotifen-treated MDA-MB-231 cells showed decreased expression of ZEB1 and Twist1 compared with that in vehicle-treated cells. Furthermore, in the primary tumors of pizotifen-treated mice, only ZEB1 expression was decreased compared with those of vehicle-treated mice. These results indicate that HTR2C-mediated signaling induced EMT through up-regulation of ZEB1 and blocking HTR2C with pizotifen induced mesenchymal-to-epithelial transition through down-regulation of ZEB1 (***Figure 5—figure supplement 4***).

We further investigated the mechanism of action of how blocking HTR2C with pizotifen induced down-regulation of ZEB1. In embryogenesis, serotonin-mediated signaling is required for Wnt-dependent specification of the superficial mesoderm during gastrulation (***Beyer et al., 2012***). Wnt signaling plays critical role in inducing EMT. In cancer cells, overexpression of HTR1D is associated with Wnt signaling (***Sui et al., 2015***; ***Zhan et al., 2017***). This evidence led to a hypothesis that HTR2C-mediated signaling might turn on transcriptional activity of β-catenin and that might induce up-regulation of EMT-TFs. IF analyses revealed β-catenin was accumulated in the nucleus of HTR2C-expressing MCF7 cells but it was located in the cytoplasm of vector control-expressing cells (***Figure 5E***). Nuclear accumulation of β-catenin in HTR2C-expressing MCF7 cells was confirmed by western blot (***Figure 5F*** and ***Figure 5—figure supplement 2***). In contrast, pizotifen-treated MDA-MB-231 cells showed β-catenin located in the cytoplasm of the cells. Vehicle-treated cells showed that β-catenin accumulated in the nucleus of the cells. (***Figure 5G***), and western blotting analysis confirmed that it was located in the cytoplasm of pizotifen-treated MDA-MB-231 cells (***Figure 5H*** and ***Figure 5—figure supplement 5***). Furthermore, immunohistochemistry and western blotting analyses showed that β-catenin accumulated in the nucleus, and phospho-GSKβ and ZEB1 expression were decreased in 4T1 primary tumors from pizotifen-treated mice compared with vehicle-treated mice (***Figure 5C*** and ***Figure 5—figure supplement 1***). These results indicated that HTR2C would regulate transcriptional activity of β-catenin and pizotifen could inhibit it.

Taken together, we conclude that blocking HTR2C with pizotifen restored epithelial properties to metastatic cells (MDA-MB-231 and 4T1 cells) through a decrease of transcriptional activity of β-catenin and that suppressed metastatic progression of the cells.

Discussion

Reducing or eliminating mortality associated with metastatic disease is a key goal of medical oncology, but few models exist that allow for rapid, effective screening of novel compounds that target the metastatic dissemination of cancer cells. Based on accumulated evidence that at least 50 genes play an essential role in governing both metastasis and gastrulation progression (***Table 1***), we hypothesized that small molecule inhibitors that interrupt gastrulation of zebrafish embryos might suppress

metastatic progression of human cancer cells. We created a unique screening concept utilizing gastrulation of zebrafish embryos to test the hypothesis. Our results clearly confirmed our hypothesis: 25.6% (20/76 drugs) of epiboly-interrupting drugs could also suppress cell motility and invasion of highly metastatic human cell lines in vitro. In particular, pizotifen, which is an antagonist for serotonin receptor 2C and one of the epiboly-interrupting drugs, could suppress metastasis in a mouse model (***Figure 3A–E***). Thus, this screen could offer a novel platform for discovery of anti-metastasis drugs.

Among the 20 drugs which suppressed both epiboly progression and cell motility and invasion of MDA-MB-231 cells, hexachlorophene and troglitazone showed the strongest effect on suppressing cell motility and invasion of MDA-MB-231 cells. However, the drug could not suppress cell motility and invasion of other highly metastatic human cancer cell lines: MDA-MB-435 and PC3. With the exception of pizotifen and S(-)eticlopride hydrochloride, the remaining 18 drugs could not show the suppressor effect on more than three highly metastatic human cancer cell lines. These results indicate that the strength of interrupting effect of a drug on epiboly progression is not proportional to the strength of suppressing effect of the drug on metastasis.

We have provided the first evidence that HTR2C, which is a primary target of pizotifen, induced EMT and promoted metastatic dissemination of cancer cells (***Figure 4A–E***). Clinical data shows that HTR2C expression is correlated with tumor stage of breast cancer patients and is higher in metastatic and Her2/neu-overexpressing tumors (***Pai et al., 2009***). That would support our finding.

Pharmacological inhibition of DRD2 with S(-)eticlopride hydrochloride suppressed cell invasion and migration of multiple human cancer cell lines in vitro. However, overexpression of DRD2 could not induce EMT on MCF7 cells. Therefore, we stopped focusing on DRD2 and S(-)eticlopride hydrochloride.

There are at least two advantages to the screen described herein. One is that the screen can easily be converted to a chemical genetic screening platform. Indeed, our screen succeeded to identify HTR2C as an EMT inducer (***Figure 4A–E***). In this research, 1280 FDA approval drugs were screened, this is less than a few percent of all of druggable targets (approximately 100 targets) in the human proteome in the body. If chemical genetic screening using specific inhibitor libraries were conducted, more genes that contribute to metastasis and gastrulation could be identified. The second advantage is that the screen enables one researcher to test 100 drugs in 5 hr with using optical microscopy, drugs, and zebrafish embryos. That indicates this screen is not only highly efficient, low-cost, and low-labor but also enables researchers who do not have high-throughput screening instruments to conduct drug screening for anti-metastasis drugs.

Materials and methods

Key resources table

Reagent type (species) or resource	Designation	Source or reference	Identifiers	Additional information
Strain, strain background (Zebrafish)	AB line	National University of Singapore		
Strain, strain background (Zebrafish)	*Tg (kdrl:eGFP)* zebrafish	Provided by Dr Stainier		
Strain, strain background (*Mus musculus*)	BALB/c	Charles River Laboratories		
Cell line (*Homo sapiens*)	MDA-MB-231	ATCC	HTB-26	
Cell line (*Homo sapiens*)	MCF7	ATCC	HTB-22	
Cell line (*Homo sapiens*)	MDA-MB-435	ATCC	HTB-129	
Cell line (*Homo sapiens*)	MIA-PaCa2	ATCC	CRM-CRL-1420	
Cell line (*Homo sapiens*)	PC3	ATCC	CRL-3471	
Cell line (*Homo sapiens*)	SW620	ATCC	CCL-227	
Cell line (*Homo sapiens*)	PC9	RIKEN BRC	RCB0446	
Cell line (*Homo sapiens*)	HaCaT	CLI	300493	

Continued on next page

Continued

Reagent type (species) or resource	Designation	Source or reference	Identifiers	Additional information
Cell line (BALB/c Mus)	4T1-12B	Provided from Dr Gary Sahagian		
Antibody	PRMT1 (A33) (Rabbit polyclonal)	Cell Signaling Technology	Cat#_2449	WB (1:1000)
Antibody	CYP11A1 (D8F4F) (Rabbit polyclonal)	Cell Signaling Technology	Cat#_14217	WB (1:1000)
Antibody	E-cadherin (4A2) (Mouse monoclonal)	Cell Signaling Technology	Cat#_14472	WB (1:1000) IF (1:100)
Antibody	EpCAM (VU1D9) (Mouse monoclonal)	Cell Signaling Technology	Cat#_2929	WB (1:1000) IF (1:100)
Antibody	Vimentin (D21H3) (Rabbit polyclonal)	Cell Signaling Technology	Cat#_5741	WB (1:1000) IF (1:100)
Antibody	N-cadherin (D4R1H) (Rabbit polyclonal)	Cell Signaling Technology	Cat#_13116	WB (1:1000) IF (1:100)
Antibody	ZEB1 (D80D3) (Rabbit polyclonal)	Cell Signaling Technology	Cat#_3396	WB (1:1000)
Antibody	Histone H3 (D1H2) (Rabbit polyclonal)	Cell Signaling Technology	Cat#_4499	WB (1:1000)
Antibody	β-Tubulin (9F3) (Rabbit polyclonal)	Cell Signaling Technology	Cat#_2128	WB (1:1000)
Antibody	GAPDH (14C10) (Rabbit polyclonal)	Cell Signaling Technology	Cat#_2118	WB (1:1000)
Antibody	HTR2C (ab133570) (Rabbit polyclonal)	Abcam	Cat#_ab133570	WB (1:1000)
Antibody	DRD2 (ab85367) (Rabbit polyclonal)	Abcam	Cat#_ab85367	WB (1:1000)
Antibody	Phospho-GSK3β (Ser9) (F-2) (Mouse monoclonal)	Santa Cruz Biotechnology	Cat#_sc-373800	WB (1:1000)
Antibody	GSK3β (1F7) (Mouse monoclonal)	Santa Cruz Biotechnology	Cat#_sc-53931	WB (1:1000)
Antibody	KRT18 (DC-10) (Mouse monoclonal)	Santa Cruz Biotechnology	Cat#_sc-6259	WB (1:1000)
Antibody	KRT19 (A53-B/A2) (Mouse monoclonal)	Santa Cruz Biotechnology	Cat#_sc-6278	WB (1:1000)
Antibody	MMP1 (3B6) (Mouse monoclonal)	Santa Cruz Biotechnology	Cat#_sc-21731	WB (1:1000)
Antibody	MMP2 (8B4) (Mouse monoclonal)	Santa Cruz Biotechnology	Cat#_sc-13595	WB (1:1000)
Antibody	S100A4 (A-7) (Mouse monoclonal)	Santa Cruz Biotechnology	Cat#_sc-377059	WB (1:1000)
Antibody	Luciferase (C-12) (Mouse monoclonal)	Santa Cruz Biotechnology	Cat#_sc-74548	WB (1:1000)
Antibody	ki67 (ki-67) (Mouse monoclonal)	Santa Cruz Biotechnology	Cat#_sc-23900	WB (1:1000)
Antibody	β-Catenin (E-5) (Mouse monoclonal)	Santa Cruz Biotechnology	Cat#_sc-7963	WB (1:1000) IF (1:100)
Antibody	FITC-conjugated E-cadherin antibody (67A4)	Biolegend	Cat#_324104	FACS (1:100)

Continued on next page

Continued

Reagent type (species) or resource	Designation	Source or reference	Identifiers	Additional information
Antibody	Anti-mouse anti-rabbit immunoglobulin G (IgG) antibodies conjugated to Alexa Fluor 488	Life Technologies	A-11029	IF (1:100)
Antibody	Anti-goat anti-rabbit immunoglobulin G (IgG) antibodies conjugated to Alexa Fluor 488	Life Technologies	A-11034	IF (1:100)
Recombinant DNA reagent	pLVX-shRNA1	Clontech	Cat#_ 632,177	
Recombinant DNA reagent	pCDH-CMV-MCS-EF1α-Hygro	System Biosciences	Cat#_CD515B-1	Gene expression vector
Recombinant DNA reagent	pMDLg/pRRE	Addgene	Addgene Plasmid #12251 RRID:Addgene_12251	Lentivirus packaging vector
Recombinant DNA reagent	pRSV-rev	Addgene	Addgene Plasmid #12253 RRID:Addgene_12253	Lentivirus packaging vector
Recombinant DNA reagent	pMD2.G	Addgene	Addgene Plasmid #12259 RRID:Addgene_12259	Lentivirus packaging vector
Recombinant DNA reagent	Providing pCMV-h5TH2C-VSV	Provided from Dr Herrick		
Chemical compound, drug	FDA-approved chemical libraries	Prestwick Chemical		
Chemical compound, drug	Pizotifen	Santa Cruz Biotechnology	Cat#_sc-201143	
Chemical compound, drug	S(-)Eticlopride hydrochloride	Santa Cruz Biotechnology	Cat#_E101	
Software, algorithm	GraphPad Prism7	GraphPad Software Inc	RRID:SCR_002798	Data analysis
Software, algorithm	FlowJo	BD Biosciences	RRID:SCR_008520	FACS data analysis

Zebrafish embryo screening

Zebrafish embryos at two-cell stage were collected at 20 min after their fertilization. Each drug was added to a well of a 24-well plate containing approximately 20 zebrafish embryos per well in either 10 or 50 μM final concentration when the embryos reached the sphere stage. Chemical treatment was initiated at 4 hpf and approximately 20 embryos were treated with two different concentrations for each compound tested. The treatment was ended at 9 hpf when vehicle- (DMSO) treated embryos as control reach 80–90% completion of the epiboly stage. The compounds which induced delay (<50% epiboly) in epiboly were selected as hit compounds for in vitro testing using highly metastatic human cancer cell lines. The study protocol was approved by the Institutional Animal Care and Use Committee of the National University of Singapore (protocol number: R16-1068).

Reagents

FDA, EMA, and other agencies-approved chemical libraries were purchased from Prestwick Chemical (Illkirch, France). Pizotifen (sc-201143) and S(-)eticlopride hydrochloride (E101) were purchased from Santa Cruz (Dallas, TX) and Sigma-Aldrich (St Louis, MO).

Cell culture and cell viability assay

MCF7, MDA-MB-231, MDA-MB-435, MIA-PaCa2, PC3, SW620, PC9, and HaCaT cells were obtained from American Type Culture Collection (ATCC, Manassas, VA). Luciferase-expressing 4T1 (4T1-12B) cells were provided from Dr Gary Sahagian (Tufts University, Boston, MA). All culture methods followed the supplier's instruction. Cell viability assay was performed as previously described (***Nakayama et al., 2020***). PCR-based mycoplasma testing on these cells was performed once in 4 months.

Plasmid

A DNA fragment coding for HTR2C was amplified by PCR with primers containing restriction enzyme recognition sequences. The HTR2C coding fragment was amplified from hsp70l:mCherry-T2A-CreERT2 plasmid (***Huang et al., 2012***).

Immunoblotting

Western blotting was performed as described previously (***Nakayama et al., 2020***). Raw data of images of western blotting analyses are uploaded as source data for western. Anti-PRMT1 (A33), anti-CYP11A1 (D8F4F), anti-E-cadherin (4A2), anti-EpCAM (VU1D9), anti-vimentin (D21H3), anti-N-cadherin (D4R1H), anti-ZEB1 (D80D3), anti-histone H3 (D1H2), anti-β-tubulin (9F3), and anti-GAPDH (14C10) antibodies were purchased from Cell Signaling Technology (Danvers, MA). Anti-HTR2C (ab133570) and anti-DRD2 (ab85367) antibodies were purchased form Abcam (Cambridge, UK). Anti-phospho-GSK3β (Ser9) (F-2), anti-GSK3β (1F7), anti-KRT18 (DC-10), anti-KRT19 (A53-B/A2), anti-MMP1 (3B6), anti-MMP2 (8B4), anti-S100A4 (A-7), anti-luciferase (C-12), anti-ki67 (ki-67), and anti-β-catenin (E-5) antibodies were purchased from Santa Cruz Biotechnology (Dallas, TX).

Flow cytometry

Cells were stained with FITC-conjugated E-cadherin antibody (67A4, Biolegend, San Diego, CA). Flow cytometry was performed as described (***Nakayama et al., 2009***) and analyzed with FlowJo software (TreeStar, Ashland, OR).

shRNA-mediated gene knockdown

The shRNA-expressing lentivirus vectors were constructed using pLVX-shRNA1 vector (632177, TAKARA Bio, Shiga, Japan). PRMT1-shRNA_#3-targeting sequence is GTGTTCCAGTATCTCTGATTA; PRMT1-shRNA_#4-targeting sequence is TTGACTCCTACGCACACTTTG. CYP11A1-shRNA_#4-targeting sequence is GCGATTCATTGATGCCATCTA; CYP11A1-shRNA_#4-targeting sequence is GAAATCCAACACCTCAGCGAT. Human HTR2C-shRNA-targeting sequence is TCATGCACCTCT GCGCTATAT. Mouse HTR2C-shRNA-targeting sequence is CTTCATACCGCTGACGATTAT. LacZ-shRNA-targeting sequence is CTACACAAATCAGCGATT.

Immunofluorescence

IF microscopy assay was performed as previously described (***Nakayama et al., 2020***). Goat anti-mouse and goat anti-rabbit immunoglobulin G (IgG) antibodies conjugated to Alexa Fluor 488 (A-11029 and A-11034, Life Technologies, Carlsbad, CA) and diluted at 1:100 were used. Nuclei were visualized by the addition of 2 μg/ml of 4′,6-diamidino-2-phenylindole (DAPI) (62248, Thermo Fisher, Waltham, MA) and photographed at 100× magnification by a fluorescent microscope BZ-X700 (KEYENCE, Osaka, Japan).

Boyden chamber cell motility and invasion assay

These assays were performed as previously described (***Nakayama et al., 2020***). In Boyden chamber assay, either 3×10^5 MDA-MB-231, 1×10^6 MDA-MB-435 or 5×10^5 PC9 cells were applied to each well in the upper chamber.

Zebrafish xenotransplantation model

Tg(kdrl:eGFP) zebrafish was provided by Dr Stainier (Max Planck Institute for Heart and Lung Research). Embryos that were derived from the line were maintained in E3 medium containing 200 μM 1-phenyl-2-thiourea (P7629, Sigma-Aldrich, St Louis, MO). Approximately 100–400 RFP-labelled MBA-MB-231 or MIA-PaCa2 cells were injected into the duct of Cuvier of the zebrafish at 2 dpf. The fish were randomly assigned to two groups. One group was maintained in the presence of pizotifen-containing E3 medium and the other group was maintained in vehicle-containing E3 medium.

Spontaneous metastasis mouse model

4T1-12B cells (2×10^4) were injected into the #4 MFP while the mice were anesthetized. To monitor tumor growth and metastases, mice were imaged biweekly by IVIS Imaging System (ParkinElmer, Waltham, MA). The primary tumor was resected 10 days after inoculation. D-Luciferin Potassium Salt

(LUCK-100) was purchased from GoldBio (St Louis, MO). The study protocol (protocol number: BRC IACUC #110612) was approved by A*STAR (Agency for Science, Technology and Research, Singapore).

Gene set enrichment analysis

Gene expression profiles obtained from zebrafish embryos at either 50%-epiboly, shield, or 75%-epiboly stage were analyzed based on the hallmark gene sets derived from the Molecular Signatures Database (MSigDB) (***Subramanian et al., 2005***; ***Liberzon et al., 2015***). The zebrafish transcriptomic data was sourced from ***White et al., 2017***. Gene sets that were significantly enriched (FDR < 0.25) were presented with the normalized enrichment score (NES) and nominal p value. Source data files for analysis of either gene expression and enriched pathways are uploaded as GSEA ***Source data 1*** and ***2***, respectively.

Histological analysis

All OCT-embedded primary tumors, lungs, and livers of mice from the spontaneous metastasis 4T1 model were sectioned on a cryostat. Eight micron sections were taken at 500 µm intervals through the entirety of the livers and lungs. Sections were subsequently stained with hematoxylin and eosin. Metastatic lesions were counted under a microscope in each section for both lungs and livers.

Statistics

Data were analyzed by Student's t test; $p < 0.05$ was considered significant.

Acknowledgements

We sincerely appreciate Dr Joshua Collins (NIH/NIDCR) and Dr Shimada (Mie University) for helping this research. We thank Dr Herrick (Albany Medical College) for providing pCMV-h5TH2C-VSV with us. This study was funded by grants from National Medical Research Council of Singapore (R-154000547511) and Ministry of Education of Singapore (R-154000A23112) to ZG.

Additional information

Funding

Funder	Grant reference number	Author
National Medical Research Council	R-154000547511	Zhiyuan Gong
Ministry of Education - Singapore	R-154000A23112	Zhiyuan Gong

The funders had no role in study design, data collection and interpretation, or the decision to submit the work for publication.

Author contributions

Joji Nakayama, Conceptualization, Data curation, Formal analysis, Investigation, Methodology, Supervision, Validation, Visualization, Writing - original draft, Writing - review and editing; Lora Tan, Formal analysis, Investigation, Validation, Visualization; Yan Li, Data curation, Investigation; Boon Cher Goh, Hideki Makinoshima, Funding acquisition, Project administration, Resources; Shu Wang, Funding acquisition, Resources; Zhiyuan Gong, Funding acquisition, Project administration, Resources, Supervision

Author ORCIDs

Joji Nakayama http://orcid.org/0000-0003-1077-140X

Ethics

The study protocol using zebrafish was approved by the Institutional Animal Care and Use Committee of the National University of Singapore (protocol number: R16-1068). The study protocol using mice (protocol number: BRC IACUC #110612) was approved by A*STAR (Agency for Science, Technology and Research, Singapore).

Decision letter and Author response
Decision letter https://doi.org/10.7554/eLife.70151.sa1
Author response https://doi.org/10.7554/eLife.70151.sa2

Additional files

Supplementary files

- Transparent reporting form
- Source data 1. GSEA analysis of zebrafish embryos at either 50%-epiboly, shield or 75%-epiboly stage.
- Source data 2. Enriched pathways of zebrafish embryos at either 50%-epiboly, shield or 75%-epiboly stage.
- Source data 3. Raw data of western-blotting analysis.
- Source data 4. Raw data of western-blotting analysis with legends.

Data availability

All data generated or analysed during this study are included in the manuscript and supporting files.

References

Abdulghani J, Gu L, Dagvadorj A, Lutz J, Leiby B, Bonuccelli G, Lisanti MP, Zellweger T, Alanen K, Mirtti T, Visakorpi T, Bubendorf L, Nevalainen MT. 2008. Stat3 promotes metastatic progression of prostate cancer. *The American Journal of Pathology* **172**:1717–1728. DOI: https://doi.org/10.2353/ajpath.2008.071054, PMID: 18483213

Bakkers J, Kramer C, Pothof J, Quaedvlieg NEM, Spaink HP, Hammerschmidt M. 2004. Has2 is required upstream of Rac1 to govern dorsal migration of lateral cells during zebrafish gastrulation. *Development* **131**:525–537. DOI: https://doi.org/10.1242/dev.00954, PMID: 14729574

Barraclough J, Hodgkinson C, Hogg A, Dive C, Welman A. 2007. Increases in c-Yes expression level and activity promote motility but not proliferation of human colorectal carcinoma cells. *Neoplasia* **9**:745–754. DOI: https://doi.org/10.1593/neo.07442, PMID: 17898870

Batlle E, Sancho E, Monfar M. 2000. The transcription factor snail is a repressor of E-cadherin gene expression in epithelial tumour cells. *Nature Cell Biology* **2**:84–89. DOI: https://doi.org/10.1038/35000034

Besser J, Leito JTD, van der Meer DLM, Bagowski CP. 2007. Tip-1 induces filopodia growth and is important for gastrulation movements during zebrafish development. *Development, Growth & Differentiation* **49**:205–214. DOI: https://doi.org/10.1111/j.1440-169X.2007.00921.x, PMID: 17394599

Beyer T, Danilchik M, Thumberger T, Vick P, Tisler M, Schneider I, Bogusch S, Andre P, Ulmer B, Walentek P, Niesler B, Blum M, Schweickert A. 2012. Serotonin signaling is required for Wnt-dependent GRP specification and leftward flow in *Xenopus*. *Current Biology* **22**:33–39. DOI: https://doi.org/10.1016/j.cub.2011.11.027, PMID: 22177902

Castanon I, Baylies MK. 2002. A Twist in fate: evolutionary comparison of Twist structure and function. *Gene* **287**:11–22. DOI: https://doi.org/10.1016/S0378-1119(01)00893-9, PMID: 11992718

Cha YI, Kim S-H, Sepich D, Buchanan FG, Solnica-Krezel L, DuBois RN. 2006. Cyclooxygenase-1-derived PGE2 promotes cell motility via the G-protein-coupled EP4 receptor during vertebrate gastrulation. *Genes & Development* **20**:77–86. DOI: https://doi.org/10.1101/gad.1374506, PMID: 16391234

Chaffer CL, Weinberg RA. 2011. A perspective on cancer cell metastasis. *Science* **331**:1559–1564. DOI: https://doi.org/10.1126/science.1203543, PMID: 21436443

Chen M-W, Hua K-T, Kao H-J, Chi C-C, Wei L-H, Johansson G, Shiah S-G, Chen P-S, Jeng Y-M, Cheng T-Y, Lai T-C, Chang J-S, Jan Y-H, Chien M-H, Yang C-J, Huang M-S, Hsiao M, Kuo M-L. 2010. H3K9 histone methyltransferase G9a promotes lung cancer invasion and metastasis by silencing the cell adhesion molecule Ep-CAM. *Cancer Research* **70**:7830–7840. DOI: https://doi.org/10.1158/0008-5472.CAN-10-0833, PMID: 20940408

Choi SC, Han JK. 2002. *Xenopus* Cdc42 regulates convergent extension movements during gastrulation through Wnt/Ca2+ signaling pathway. *Developmental Biology* **244**:342–357. DOI: https://doi.org/10.1006/dbio.2002.0602, PMID: 11944942

Coyle RC, Latimer A, Jessen JR. 2008. Membrane-type 1 matrix metalloproteinase regulates cell migration during zebrafish gastrulation: evidence for an interaction with non-canonical Wnt signaling. *Experimental Cell Research* **314**:2150–2162. DOI: https://doi.org/10.1016/j.yexcr.2008.03.010, PMID: 18423448

Dai X, Ge J, Wang X, Qian X, Zhang C, Li X. 2013. OCT4 regulates epithelial-mesenchymal transition and its knockdown inhibits colorectal cancer cell migration and invasion. *Oncology Reports* **29**:155–160. DOI: https://doi.org/10.3892/or.2012.2086, PMID: 23076549

Damm EW, Winklbauer R. 2011. PDGF-A controls mesoderm cell orientation and radial intercalation during *Xenopus* gastrulation. *Development* **138**:565–575. DOI: https://doi.org/10.1242/dev.056903, PMID: 21205800

Dongre A, Weinberg RA. 2019. New insights into the mechanisms of epithelial-mesenchymal transition and implications for cancer. *Nature Reviews. Molecular Cell Biology* **20**:69–84. DOI: https://doi.org/10.1038/s41580-018-0080-4, PMID: 30459476

Faure S, Cau J, de Santa Barbara P, Bigou S, Ge Q, Delsert C, Morin N. 2005. *Xenopus* p21-activated kinase 5 regulates blastomeres' adhesive properties during convergent extension movements. *Developmental Biology* **277**:472–492. DOI: https://doi.org/10.1016/j.ydbio.2004.10.005, PMID: 15617688

Felding-Habermann B. 2003. Integrin adhesion receptors in tumor metastasis. *Clinical & Experimental Metastasis* **20**:203–213. DOI: https://doi.org/10.1023/a:1022983000355, PMID: 12741679

Fernando RI, Litzinger M, Trono P, Hamilton DH, Schlom J, Palena C. 2010. The T-box transcription factor Brachyury promotes epithelial-mesenchymal transition in human tumor cells. *The Journal of Clinical Investigation* **120**:533–544. DOI: https://doi.org/10.1172/JCI38379, PMID: 20071775

Gong W, An Z, Wang Y, Pan X, Fang W, Jiang B, Zhang H. 2009. P21-activated kinase 5 is overexpressed during colorectal cancer progression and regulates colorectal carcinoma cell adhesion and migration. *International Journal of Cancer* **125**:548–555. DOI: https://doi.org/10.1002/ijc.24428, PMID: 19415746

Gunaratne A, Thai BL, Di Guglielmo GM. 2013. Atypical protein kinase C phosphorylates Par6 and facilitates transforming growth factor β-induced epithelial-to-mesenchymal transition. *Molecular and Cellular Biology* **33**:874–886. DOI: https://doi.org/10.1128/MCB.00837-12, PMID: 23249950

Gunnarsson L, Jauhiainen A, Kristiansson E, Nerman O, Larsson DGJ. 2008. Evolutionary conservation of human drug targets in organisms used for environmental risk assessments. *Environmental Science & Technology* **42**:5807–5813. DOI: https://doi.org/10.1021/es8005173, PMID: 18754513

Guo BH, Feng Y, Zhang R, Xu LH, Li MZ, Kung HF, Song LB, Zeng MS. 2011. Bmi-1 promotes invasion and metastasis, and its elevated expression is correlated with an advanced stage of breast cancer. *Molecular Cancer* **10**:10. DOI: https://doi.org/10.1186/1476-4598-10-10

Habas R, Dawid IB, He X. 2003. Coactivation of Rac and Rho by Wnt/Frizzled signaling is required for vertebrate gastrulation. *Genes & Development* **17**:295–309. DOI: https://doi.org/10.1101/gad.1022203, PMID: 12533515

Han M, Wang H, Zhang HT, Han Z. 2012. The PDZ protein TIP-1 facilitates cell migration and pulmonary metastasis of human invasive breast cancer cells in athymic mice. *Biochemical and Biophysical Research Communications* **422**:139–145. DOI: https://doi.org/10.1016/j.bbrc.2012.04.123, PMID: 22564736

Hartwell KA, Muir B, Reinhardt F, Carpenter AE, Sgroi DC, Weinberg RA. 2006. The Spemann organizer gene, Goosecoid, promotes tumor metastasis. *PNAS* **103**:18969–18974. DOI: https://doi.org/10.1073/pnas.0608636103, PMID: 17142318

Holloway BA, Gomez de la Torre Canny S, Ye Y, Slusarski DC, Freisinger CM, Dosch R, Chou MM, Wagner DS, Mullins MC. 2009. A novel role for MAPKAPK2 in morphogenesis during zebrafish development. *PLOS Genetics* **5**:e1000413. DOI: https://doi.org/10.1371/journal.pgen.1000413, PMID: 19282986

Hong SK, Tanegashima K, Dawid IB. 2011. XIer2 is required for convergent extension movements during *Xenopus* development. *The International Journal of Developmental Biology* **55**:917–921. DOI: https://doi.org/10.1387/ijdb.113288sh, PMID: 22252488

Hsu HJ, Liang MR, Chen CT, Chung B. 2006. Pregnenolone stabilizes microtubules and promotes zebrafish embryonic cell movement. *Nature* **439**:480–483. DOI: https://doi.org/10.1038/nature04436, PMID: 16437115

Huang EW, Xue SJ, Zhang Z, Zhou JG, Guan YY, Tang YB. 2012. Vinpocetine inhibits breast cancer cells growth in vitro and in vivo. *Apoptosis : An International Journal on Programmed Cell Death* **17**:1120–1130. DOI: https://doi.org/10.1007/s10495-012-0743-0, PMID: 22729609

Iioka H, Ueno N, Kinoshita N. 2004. Essential role of MARCKS in cortical actin dynamics during gastrulation movements. *The Journal of Cell Biology* **164**:169–174. DOI: https://doi.org/10.1083/jcb.200310027, PMID: 14718521

Ip YT, Gridley T. 2002. Cell movements during gastrulation: Snail dependent and independent pathways. *Current Opinion in Genetics & Development* **12**:423–429. DOI: https://doi.org/10.1016/S0959-437X(02)00320-9, PMID: 12100887

Itoh K, Yoshioka K, Akedo H, Uehata M, Ishizaki T, Narumiya S. 1999. An essential part for Rho-associated kinase in the transcellular invasion of tumor cells. *Nature Medicine* **5**:221–225. DOI: https://doi.org/10.1038/5587, PMID: 9930872

Jechlinger M, Sommer A, Moriggl R, Seither P, Kraut N, Capodiecci P, Donovan M, Cordon-Cardo C, Beug H, Grünert S. 2006. Autocrine PDGFR signaling promotes mammary cancer metastasis. *The Journal of Clinical Investigation* **116**:1561–1570. DOI: https://doi.org/10.1172/JCI24652, PMID: 16741576

Jopling C, van Geemen D, den Hertog J. 2007. Shp2 knockdown and Noonan/LEOPARD mutant Shp2-induced gastrulation defects. *PLOS Genetics* **3**:e225. DOI: https://doi.org/10.1371/journal.pgen.0030225, PMID: 18159945

Katsuno Y, Hanyu A, Kanda H, Ishikawa Y, Akiyama F, Iwase T, Ogata E, Ehata S, Miyazono K, Imamura T. 2008. Bone morphogenetic protein signaling enhances invasion and bone metastasis of breast cancer cells through Smad pathway. *Oncogene* **27**:6322–6333. DOI: https://doi.org/10.1038/onc.2008.232, PMID: 18663362

Khanna C, Wan X, Bose S, Cassaday R, Olomu O, Mendoza A, Yeung C, Gorlick R, Hewitt SM, Helman LJ. 2004. The membrane-cytoskeleton linker ezrin is necessary for osteosarcoma metastasis. *Nature Medicine* **10**:182–186. DOI: https://doi.org/10.1038/nm982, PMID: 14704791

Kim H-R, Wheeler MA, Wilson CM, Iida J, Eng D, Simpson MA, McCarthy JB, Bullard KM. 2004. Hyaluronan facilitates invasion of colon carcinoma cells in vitro via interaction with CD44. *Cancer Research* **64**:4569–4576. DOI: https://doi.org/10.1158/0008-5472.CAN-04-0202, PMID: 15231668

Kolosionek E, Savai R, Ghofrani HA, Weissmann N, Guenther A, Grimminger F, Seeger W, Banat GA, Schermuly RT, Pullamsetti SS. 2009. Expression and activity of phosphodiesterase isoforms during epithelial mesenchymal transition: the role of phosphodiesterase 4. *Molecular Biology of the Cell* **20**:4751–4765. DOI: https://doi.org/10.1091/mbc.E09-01-0019, PMID: 19759179

Kondo M. 2007. Bone morphogenetic proteins in the early development of zebrafish. *The FEBS Journal* **274**:2960–2967. DOI: https://doi.org/10.1111/j.1742-4658.2007.05838.x, PMID: 17521339

Krens SFG, He S, Lamers GEM, Meijer AH, Bakkers J, Schmidt T, Spaink HP, Snaar-Jagalska BE. 2008. Distinct functions for ERK1 and ERK2 in cell migration processes during zebrafish gastrulation. *Developmental Biology* **319**:370–383. DOI: https://doi.org/10.1016/j.ydbio.2008.04.032, PMID: 18514184

Kröger C, Afeyan A, Mraz J, Eaton EN, Reinhardt F, Khodor YL, Thiru P, Bierie B, Ye X, Burge CB, Weinberg RA. 2019. Acquisition of a hybrid E/M state is essential for tumorigenicity of basal breast cancer cells. *PNAS* **116**:7353–7362. DOI: https://doi.org/10.1073/pnas.1812876116, PMID: 30910979

Kumar B, Koul S, Petersen J, Khandrika L, Hwa JS, Meacham RB, Wilson S, Koul HK. 2010. p38 mitogen-activated protein kinase-driven MAPKAPK2 regulates invasion of bladder cancer by modulation of MMP-2 and MMP-9 activity. *Cancer Research* **70**:832–841. DOI: https://doi.org/10.1158/0008-5472.CAN-09-2918, PMID: 20068172

Kundu N, Fulton AM. 2002. Selective cyclooxygenase (COX)-1 or COX-2 inhibitors control metastatic disease in a murine model of breast cancer. *Cancer Research* **62**:2343–2346 PMID: 11956094.,

Kusakabe M, Nishida E. 2004. The polarity-inducing kinase Par-1 controls *Xenopus* gastrulation in cooperation with 14-3-3 and aPKC. *The EMBO Journal* **23**:4190–4201. DOI: https://doi.org/10.1038/sj.emboj.7600381, PMID: 15343271

Lachnit M, Kur E, Driever W. 2008. Alterations of the cytoskeleton in all three embryonic lineages contribute to the epiboly defect of Pou5f1/Oct4 deficient MZspg zebrafish embryos. *Developmental Biology* **315**:1–17. DOI: https://doi.org/10.1016/j.ydbio.2007.10.008, PMID: 18215655

Latimer A, Jessen JR. 2010. Extracellular matrix assembly and organization during zebrafish gastrulation. *Matrix Biology* **29**:89–96. DOI: https://doi.org/10.1016/j.matbio.2009.10.002, PMID: 19840849

Latinkic BV, Mercurio S, Bennett B, Hirst EMA, Xu Q, Lau LF, Mohun TJ, Smith JC. 2003. *Xenopus* Cyr61 regulates gastrulation movements and modulates Wnt signalling. *Development* **130**:2429–2441. DOI: https://doi.org/10.1242/dev.00449, PMID: 12702657

Liberzon A, Birger C, Thorvaldsdóttir H, Ghandi M, Mesirov JP, Tamayo P. 2015. The Molecular Signatures Database (MSigDB) hallmark gene set collection. *Cell Systems* **1**:417–425. DOI: https://doi.org/10.1016/j.cels.2015.12.004, PMID: 26771021

Lin F, Sepich DS, Chen S, Topczewski J, Yin C, Solnica-Krezel L, Hamm H. 2005. Essential roles of G{alpha}12/13 signaling in distinct cell behaviors driving zebrafish convergence and extension gastrulation movements. *The Journal of Cell Biology* **169**:777–787. DOI: https://doi.org/10.1083/jcb.200501104, PMID: 15928205

Lin J, Huo R, Wang L, Zhou Z, Sun Y, Shen B, Wang R, Li N. 2012. A novel anti-Cyr61 antibody inhibits breast cancer growth and metastasis in vivo. *Cancer Immunology, Immunotherapy* **61**:677–687. DOI: https://doi.org/10.1007/s00262-011-1135-y, PMID: 22048717

Link V, Carvalho L, Castanon I, Stockinger P, Shevchenko A, Heisenberg C-P. 2006. Identification of regulators of germ layer morphogenesis using proteomics in zebrafish. *Journal of Cell Science* **119**:2073–2083. DOI: https://doi.org/10.1242/jcs.02928, PMID: 16638810

Liu W, Su L-T, Khadka DK, Mezzacappa C, Komiya Y, Sato A, Habas R, Runnels LW. 2011. TRPM7 regulates gastrulation during vertebrate embryogenesis. *Developmental Biology* **350**:348–357. DOI: https://doi.org/10.1016/j.ydbio.2010.11.034, PMID: 21145885

Liu P, Kumar IS, Brown S, Kannappan V, Tawari PE, Tang JZ, Jiang W, Armesilla AL, Darling JL, Wang W. 2013. Disulfiram targets cancer stem-like cells and reverses resistance and cross-resistance in acquired paclitaxel-resistant triple-negative breast cancer cells. *British Journal of Cancer* **109**:1876–1885. DOI: https://doi.org/10.1038/bjc.2013.534, PMID: 24008666

Lu Z, Jiang G, Blume-Jensen P, Hunter T. 2001. Epidermal growth factor-induced tumor cell invasion and metastasis initiated by dephosphorylation and downregulation of focal adhesion kinase. *Molecular and Cellular Biology* **21**:4016–4031. DOI: https://doi.org/10.1128/MCB.21.12.4016-4031.2001, PMID: 11359909

Lu W, Kang Y. 2019. Epithelial-Mesenchymal Plasticity in Cancer Progression and Metastasis. *Developmental Cell* **49**:361–374. DOI: https://doi.org/10.1016/j.devcel.2019.04.010, PMID: 31063755

Lue H-W, Yang X, Wang R, Qian W, Xu RZH, Lyles R, Osunkoya AO, Zhou BP, Vessella RL, Zayzafoon M, Liu Z-R, Zhau HE, Chung LWK. 2011. LIV-1 promotes prostate cancer epithelial-to-mesenchymal transition and metastasis through HB-EGF shedding and EGFR-mediated ERK signaling. *PLOS ONE* **6**:e27720. DOI: https://doi.org/10.1371/journal.pone.0027720, PMID: 22110740

Lynch TP, Ferrer CM, Jackson SR, Shahriari KS, Vosseller K, Reginato MJ. 2012. Critical role of O-Linked β-N-acetylglucosamine transferase in prostate cancer invasion, angiogenesis, and metastasis. *The Journal of Biological Chemistry* **287**:11070–11081. DOI: https://doi.org/10.1074/jbc.M111.302547, PMID: 22275356

Machingo QJ, Fritz A, Shur BD. 2006. A beta1,4-galactosyltransferase is required for convergent extension movements in zebrafish. *Developmental Biology* **297**:471–482. DOI: https://doi.org/10.1016/j.ydbio.2006.05.024, PMID: 16904099

Malik G, Knowles LM, Dhir R, Xu S, Yang S, Ruoslahti E, Pilch J. 2010. Plasma fibronectin promotes lung metastasis by contributions to fibrin clots and tumor cell invasion. *Cancer Research* **70**:4327–4334. DOI: https://doi.org/10.1158/0008-5472.CAN-09-3312, PMID: 20501851

Mani SA, Yang J, Brooks M, Schwaninger G, Zhou A, Miura N, Kutok JL, Hartwell K, Richardson AL, Weinberg RA. 2007. Mesenchyme Forkhead 1 (FOXC2) plays a key role in metastasis and is associated with aggressive basal-like breast cancers. *PNAS* **104**:10069–10074. DOI: https://doi.org/10.1073/pnas.0703900104, PMID: 17537911

Marlow F, Topczewski J, Sepich D, Solnica-Krezel L. 2002. Zebrafish Rho kinase 2 acts downstream of Wnt11 to mediate cell polarity and effective convergence and extension movements. *Current Biology* **12**:876–884. DOI: https://doi.org/10.1016/s0960-9822(02)00864-3, PMID: 12062050

Marsden M, DeSimone DW. 2003. Integrin-ECM interactions regulate cadherin-dependent cell adhesion and are required for convergent extension in *Xenopus*. *Current Biology* **13**:1182–1191. DOI: https://doi.org/10.1016/s0960-9822(03)00433-0, PMID: 12867028

Medici D, Hay ED, Olsen BR, Bronner-Fraser M. 2008. Snail and Slug Promote Epithelial-Mesenchymal Transition through β-Catenin–T-Cell Factor-4-dependent Expression of Transforming Growth Factor-β3. *Molecular Biology of the Cell* **19**:4875–4887. DOI: https://doi.org/10.1091/mbc.e08-05-0506, PMID: 18799618

Middelbeek J, Kuipers AJ, Henneman L, Visser D, Eidhof I, van Horssen R, Wieringa B, Canisius SV, Zwart W, Wessels LF, Sweep FCGJ, Bult P, Span PN, van Leeuwen FN, Jalink K. 2012. TRPM7 is required for breast tumor cell metastasis. *Cancer Research* **72**:4250–4261. DOI: https://doi.org/10.1158/0008-5472.CAN-11-3863, PMID: 22871386

Miyagi C, Yamashita S, Ohba Y, Yoshizaki H, Matsuda M, Hirano T. 2004. STAT3 noncell-autonomously controls planar cell polarity during zebrafish convergence and extension. *The Journal of Cell Biology* **166**:975–981. DOI: https://doi.org/10.1083/jcb.200403110, PMID: 15452141

Mizoguchi T, Verkade H, Heath JK, Kuroiwa A, Kikuchi Y. 2008. Sdf1/Cxcr4 signaling controls the dorsal migration of endodermal cells during zebrafish gastrulation. *Development* **135**:2521–2529. DOI: https://doi.org/10.1242/dev.020107, PMID: 18579679

Montero JA, Kilian B, Chan J, Bayliss PE, Heisenberg CP. 2003. Phosphoinositide 3-kinase is required for process outgrowth and cell polarization of gastrulating mesendodermal cells. *Current Biology* **13**:1279–1289. DOI: https://doi.org/10.1016/s0960-9822(03)00505-0, PMID: 12906787

Nakayama J, Yamamoto M, Hayashi K, Satoh H, Bundo K, Kubo M, Goitsuka R, Farrar MA, Kitamura D. 2009. BLNK suppresses pre-B-cell leukemogenesis through inhibition of JAK3. *Blood* **113**:1483–1492. DOI: https://doi.org/10.1182/blood-2008-07-166355, PMID: 19047679

Nakayama J, Lu JW, Makinoshima H, Gong Z. 2020. A Novel Zebrafish Model of Metastasis Identifies the HSD11β1 Inhibitor Adrenosterone as a Suppressor of Epithelial-Mesenchymal Transition and Metastatic Dissemination. *Molecular Cancer Research* **18**:477–487. DOI: https://doi.org/10.1158/1541-7786.MCR-19-0759, PMID: 31748280

Neeb A, Wallbaum S, Novac N, Dukovic-Schulze S, Scholl I, Schreiber C, Schlag P, Moll J, Stein U, Sleeman JP. 2012. The immediate early gene Ier2 promotes tumor cell motility and metastasis, and predicts poor survival of colorectal cancer patients. *Oncogene* **31**:3796–3806. DOI: https://doi.org/10.1038/onc.2011.535, PMID: 22120713

Nguyen DX, Bos PD, Massagué J. 2009. Metastasis: from dissemination to organ-specific colonization. *Nature Reviews. Cancer* **9**:274–284. DOI: https://doi.org/10.1038/nrc2622, PMID: 19308067

Ni J, Cozzi PJ, Duan W, Shigdar S, Graham PH, John KH, Li Y. 2012. Role of the EpCAM (CD326) in prostate cancer metastasis and progression. *Cancer Metastasis Reviews* **31**:779–791. DOI: https://doi.org/10.1007/s10555-012-9389-1, PMID: 22718399

Nieto MA, Huang RYJ, Jackson RA, Thiery JP. 2016. EMT: 2016. *Cell* **166**:21–45. DOI: https://doi.org/10.1016/j.cell.2016.06.028, PMID: 27368099

Nomura S, Yoshitomi H, Takano S, Shida T, Kobayashi S, Ohtsuka M, Kimura F, Shimizu H, Yoshidome H, Kato A, Miyazaki M. 2008. FGF10/FGFR2 signal induces cell migration and invasion in pancreatic cancer. *British Journal of Cancer* **99**:305–313. DOI: https://doi.org/10.1038/sj.bjc.6604473, PMID: 18594526

O'Carroll D, Erhardt S, Pagani M, Barton SC, Surani MA, Jenuwein T. 2001. The polycomb-group gene Ezh2 is required for early mouse development. *Molecular and Cellular Biology* **21**:4330–4336. DOI: https://doi.org/10.1128/MCB.21.13.4330-4336.2001, PMID: 11390661

Pai VP, Marshall AM, Hernandez LL, Buckley AR, Horseman ND. 2009. Altered serotonin physiology in human breast cancers favors paradoxical growth and cell survival. *Breast Cancer Research* **11**:bcr2448. DOI: https://doi.org/10.1186/bcr2448

Perentes JY, Kirkpatrick ND, Nagano S, Smith EY, Shaver CM, Sgroi D, Garkavtsev I, Munn LL, Jain RK, Boucher Y. 2011. Cancer cell-associated MT1-MMP promotes blood vessel invasion and distant metastasis in triple-negative mammary tumors. *Cancer Research* **71**:4527–4538. DOI: https://doi.org/10.1158/0008-5472.CAN-10-4376, PMID: 21571860

Radtke S, Milanovic M, Rossé C, De Rycker M, Lachmann S, Hibbert A, Kermorgant S, Parker PJ. 2013. ERK2 but not ERK1 mediates HGF-induced motility in non-small cell lung carcinoma cell lines. *Journal of Cell Science* **126**:2381–2391. DOI: https://doi.org/10.1242/jcs.115832, PMID: 23549785

Ren G, Baritaki S, Marathe H, Feng J, Park S, Beach S, Bazeley PS, Beshir AB, Fenteany G, Mehra R, Daignault S, Al-Mulla F, Keller E, Bonavida B, de la Serna I, Yeung KC. 2012. Polycomb protein EZH2 regulates tumor invasion via the transcriptional repression of the metastasis suppressor RKIP in breast and prostate cancer. *Cancer Research* **72**:3091–3104. DOI: https://doi.org/10.1158/0008-5472.CAN-11-3546, PMID: 22505648

Reymond N, Im JH, Garg R, Vega FM, Borda d'Agua B, Riou P, Cox S, Valderrama F, Muschel RJ, Ridley AJ. 2012. Cdc42 promotes transendothelial migration of cancer cells through β1 integrin. *The Journal of Cell Biology* **199**:653–668. DOI: https://doi.org/10.1083/jcb.201205169, PMID: 23148235

Rombouts K, Carloni V, Mello T, Omenetti S, Galastri S, Madiai S, Galli A, Pinzani M. 2013. Myristoylated Alanine-Rich protein Kinase C Substrate (MARCKS) expression modulates the metastatic phenotype in human and murine colon carcinoma in vitro and in vivo. *Cancer Letters* **333**:244–252. DOI: https://doi.org/10.1016/j.canlet.2013.01.040, PMID: 23376641

Sack U, Walther W, Scudiero D, Selby M, Kobelt D, Lemm M, Fichtner I, Schlag PM, Shoemaker RH, Stein U. 2011. Novel effect of antihelminthic Niclosamide on S100A4-mediated metastatic progression in colon cancer. *Journal of the National Cancer Institute* **103**:1018–1036. DOI: https://doi.org/10.1093/jnci/djr190, PMID: 21685359

Sander V, Reversade B, De Robertis EM. 2007. The opposing homeobox genes Goosecoid and Vent1/2 self-regulate *Xenopus* patterning. *The EMBO Journal* **26**:2955–2965. DOI: https://doi.org/10.1038/sj.emboj.7601705, PMID: 17525737

Sasaki T, Kuniyasu H, Luo Y, Fujiwara R, Kitayoshi M, Tanabe E, Kato D, Shinya S, Fujii K, Ohmori H, Yamashita Y. 2014. Serum CD10 is associated with liver metastasis in colorectal cancer. *The Journal of Surgical Research* **192**:390–394. DOI: https://doi.org/10.1016/j.jss.2014.05.071, PMID: 24972738

Seifert K, Ibrahim H, Stodtmeister T, Winklbauer R, Niessen CM. 2009. An adhesion-independent, aPKC-dependent function for cadherins in morphogenetic movements. *Journal of Cell Science* **122**:2514–2523. DOI: https://doi.org/10.1242/jcs.042796, PMID: 19549688

Sharma D, Holets L, Zhang X, Kinsey WH. 2005. Role of Fyn kinase in signaling associated with epiboly during zebrafish development. *Developmental Biology* **285**:462–476. DOI: https://doi.org/10.1016/j.ydbio.2005.07.018, PMID: 16112104

Shen H, Gu Z, Jian K, Qi J. 2013. CXCR4-mediated Stat3 activation is essential for CXCL12-induced cell invasion in bladder cancer. *Tumour Biology* **34**:1839–1845. DOI: https://doi.org/10.1007/s13277-013-0725-z, PMID: 23526079

Shi X, Gangadharan B, Brass LF, Ruf W, Mueller BM. 2004. Protease-activated receptors (PAR1 and PAR2) contribute to tumor cell motility and metastasis. *Molecular Cancer Research* **2**:395–402 PMID: 15280447.,

Shi J, Severson C, Yang J, Wedlich D, Klymkowsky MW. 2011. Snail2 controls mesodermal BMP/Wnt induction of neural crest. *Development* **138**:3135–3145. DOI: https://doi.org/10.1242/dev.064394, PMID: 21715424

Skalski M, Alfandari D, Darribère T. 1998. A key function for alphav containing integrins in mesodermal cell migration during Pleurodeles waltl gastrulation. *Developmental Biology* **195**:158–173. DOI: https://doi.org/10.1006/dbio.1997.8838, PMID: 9520332

Slanchev K, Carney TJ, Stemmler MP, Koschorz B, Amsterdam A, Schwarz H, Hammerschmidt M. 2009. The epithelial cell adhesion molecule EpCAM is required for epithelial morphogenesis and integrity during zebrafish epiboly and skin development. *PLOS Genetics* **5**:e1000563. DOI: https://doi.org/10.1371/journal.pgen.1000563, PMID: 19609345

Solnica-Krezel L. 2005. Conserved patterns of cell movements during vertebrate gastrulation. *Current Biology* **15**:R213–R228. DOI: https://doi.org/10.1016/j.cub.2005.03.016, PMID: 15797016

Solnica-Krezel L. 2006. Gastrulation in zebrafish -- all just about adhesion? *Current Opinion in Genetics & Development* **16**:433–441. DOI: https://doi.org/10.1016/j.gde.2006.06.009, PMID: 16797963

Song S, Eckerle S, Onichtchouk D, Marrs JA, Nitschke R, Driever W. 2013. Pou5f1-dependent EGF expression controls E-cadherin endocytosis, cell adhesion, and zebrafish epiboly movements. *Developmental Cell* **24**:486–501. DOI: https://doi.org/10.1016/j.devcel.2013.01.016, PMID: 23484854

Spaderna S, Schmalhofer O, Wahlbuhl M, Dimmler A, Bauer K, Sultan A, Hlubek F, Jung A, Strand D, Eger A, Kirchner T, Behrens J, Brabletz T. 2008. The transcriptional repressor ZEB1 promotes metastasis and loss of cell polarity in cancer. *Cancer Research* **68**:537–544. DOI: https://doi.org/10.1158/0008-5472.CAN-07-5682, PMID: 18199550

Speirs CK, Jernigan KK, Kim S-H, Cha YI, Lin F, Sepich DS, DuBois RN, Lee E, Solnica-Krezel L. 2010. Prostaglandin Gbetagamma signaling stimulates gastrulation movements by limiting cell adhesion through Snai1a stabilization. *Development* **137**:1327–1337. DOI: https://doi.org/10.1242/dev.045971, PMID: 20332150

Subramanian A, Tamayo P, Mootha VK, Mukherjee S, Ebert BL, Gillette MA, Paulovich A, Pomeroy SL, Golub TR, Lander ES, Mesirov JP. 2005. Gene set enrichment analysis: a knowledge-based approach for interpreting genome-wide expression profiles. *PNAS* **102**:15545–15550. DOI: https://doi.org/10.1073/pnas.0506580102, PMID: 16199517

Sui H, Xu H, Ji Q, Liu X, Zhou L, Song H, Zhou X, Xu Y, Chen Z, Cai J, Ji G, Li Q. 2015. 5-hydroxytryptamine receptor (5-HT1DR) promotes colorectal cancer metastasis by regulating Axin1/β-catenin/MMP-7 signaling pathway. *Oncotarget* **6**:25975–25987. DOI: https://doi.org/10.18632/oncotarget.4543, PMID: 26214021

Szilágyi G, Nagy Z, Balkay L, Boros I, Emri M, Lehel S, Márián T, Molnár T, Szakáll S, Trón L, Bereczki D, Csiba L, Fekete I, Kerényi L, Galuska L, Varga J, Bönöczk P, Vas A, Gulyás B. 2005. Effects of vinpocetine on the redistribution of cerebral blood flow and glucose metabolism in chronic ischemic stroke patients: a PET study. *Journal of the Neurological Sciences* **229–230**:275–284. DOI: https://doi.org/10.1016/j.jns.2004.11.053, PMID: 15760651

Tada M, Smith JC. 2000. Xwnt11 is a target of *Xenopus* Brachyury: regulation of gastrulation movements via Dishevelled, but not through the canonical Wnt pathway. *Development* **127**:2227–2238. DOI: https://doi.org/10.1242/dev.127.10.2227, PMID: 10769246

Tao K, Fang M, Alroy J, Sahagian GG. 2008. Imagable 4T1 model for the study of late stage breast cancer. *BMC Cancer* **8**:228. DOI: https://doi.org/10.1186/1471-2407-8-228, PMID: 18691423

Thiery JP, Acloque H, Huang RYJ, Nieto MA. 2009. Epithelial-Mesenchymal Transitions in Development and Disease. *Cell* **139**:871–890. DOI: https://doi.org/10.1016/j.cell.2009.11.007

Tsai WB, Zhang X, Sharma D, Wu W, Kinsey WH. 2005. Role of Yes kinase during early zebrafish development. *Developmental Biology* **277**:129–141. DOI: https://doi.org/10.1016/j.ydbio.2004.08.052, PMID: 15572145

Tsai Y-J, Pan H, Hung C-M, Hou P-T, Li Y-C, Lee Y-J, Shen Y-T, Wu T-T, Li C. 2011. The predominant protein arginine methyltransferase PRMT1 is critical for zebrafish convergence and extension during gastrulation. *The FEBS Journal* **278**:905–917. DOI: https://doi.org/10.1111/j.1742-4658.2011.08006.x, PMID: 21214862

Tsai JH, Yang J. 2013. Epithelial-mesenchymal plasticity in carcinoma metastasis. *Genes & Development* **27**:2192–2206. DOI: https://doi.org/10.1101/gad.225334.113, PMID: 24142872

van der Lugt NM, Domen J, Linders K, van Roon M, Robanus-Maandag E, te Riele H, van der Valk M, Deschamps J, Sofroniew M, van Lohuizen M. 1994. Posterior transformation, neurological abnormalities, and severe hematopoietic defects in mice with a targeted deletion of the bmi-1 proto-oncogene. *Genes & Development* **8**:757–769. DOI: https://doi.org/10.1101/gad.8.7.757, PMID: 7926765

Vannier C, Mock K, Brabletz T, Driever W. 2013. Zeb1 regulates E-cadherin and Epcam (epithelial cell adhesion molecule) expression to control cell behavior in early zebrafish development. *The Journal of Biological Chemistry* **288**:18643–18659. DOI: https://doi.org/10.1074/jbc.M113.467787, PMID: 23667256

Vega FM, Ridley AJ. 2008. Rho GTPases in cancer cell biology. *FEBS Letters* **582**:2093–2101. DOI: https://doi.org/10.1016/j.febslet.2008.04.039, PMID: 18460342

Vincan E, Barker N. 2008. The upstream components of the Wnt signalling pathway in the dynamic EMT and MET associated with colorectal cancer progression. *Clinical & Experimental Metastasis* **25**:657–663. DOI: https://doi.org/10.1007/s10585-008-9156-4, PMID: 18350253

Wander SA, Zhao D, Besser AH, Hong F, Wei J, Ince TA, Milikowski C, Bishopric NH, Minn AJ, Creighton CJ, Slingerland JM. 2013. PI3K/mTOR inhibition can impair tumor invasion and metastasis in vivo despite a lack of antiproliferative action in vitro: implications for targeted therapy. *Breast Cancer Research and Treatment* **138**:369–381. DOI: https://doi.org/10.1007/s10549-012-2389-6, PMID: 23430223

Wang F, Liu H, Liu S, Tang S, Yang L, Feng G. 2005. SHP-2 promoting migration and metastasis of MCF-7 with loss of E-cadherin, dephosphorylation of FAK and secretion of MMP-9 induced by IL-1beta in vivo and in vitro. *Breast Cancer Research and Treatment* **89**:5–14. DOI: https://doi.org/10.1007/s10549-004-1002-z, PMID: 15666191

Wang D, Dubois RN. 2006. Prostaglandins and cancer. *Gut* **55**:115–122. DOI: https://doi.org/10.1136/gut.2004.047100, PMID: 16118353

Webster DM, Teo CF, Sun Y, Wloga D, Gay S, Klonowski KD, Wells L, Dougan ST. 2009. O-GlcNAc modifications regulate cell survival and epiboly during zebrafish development. *BMC Developmental Biology* **9**:28. DOI: https://doi.org/10.1186/1471-213X-9-28, PMID: 19383152

Weinbach EC, Garbus J. 1969. Mechanism of action of reagents that uncouple oxidative phosphorylation. *Nature* **221**:1016–1018. DOI: https://doi.org/10.1038/2211016a0, PMID: 4180173

Welch DR, Hurst DR. 2019. Defining the Hallmarks of Metastasis. *Cancer Research* **79**:3011–3027. DOI: https://doi.org/10.1158/0008-5472.CAN-19-0458

White RJ, Collins JE, Sealy IM, Wali N, Dooley CM, Digby Z, Stemple DL, Murphy DN, Billis K, Hourlier T, Füllgrabe A, Davis MP, Enright AJ, Busch-Nentwich EM. 2017. A high-resolution mRNA expression time course of embryonic development in zebrafish. *eLife* **6**:e30860. DOI: https://doi.org/10.7554/eLife.30860, PMID: 29144233

Wilm B, James RG, Schultheiss TM, Hogan BLM. 2004. The forkhead genes, Foxc1 and Foxc2, regulate paraxial versus intermediate mesoderm cell fate. *Developmental Biology* **271**:176–189. DOI: https://doi.org/10.1016/j.ydbio.2004.03.034, PMID: 15196959

Yadav V, Denning MF. 2011. Fyn is induced by Ras/PI3K/Akt signaling and is required for enhanced invasion/migration. *Molecular Carcinogenesis* **50**:346–352. DOI: https://doi.org/10.1002/mc.20716, PMID: 21480388

Yagi H, Tan W, Dillenburg-Pilla P, Armando S, Amornphimoltham P, Simaan M, Weigert R, Molinolo AA, Bouvier M, Gutkind JS. 2011. A synthetic biology approach reveals a CXCR4-G13-Rho signaling axis driving transendothelial migration of metastatic breast cancer cells. *Science Signaling* **4**:ra60. DOI: https://doi.org/10.1126/scisignal.2002221, PMID: 21934106

Yamashita S, Miyagi C, Fukada T, Kagara N, Che Y-S, Hirano T. 2004. Zinc transporter LIVI controls epithelial-mesenchymal transition in zebrafish gastrula organizer. *Nature* **429**:298–302. DOI: https://doi.org/10.1038/nature02545, PMID: 15129296

Yamazaki K, Takamura M, Masugi Y, Mori T, Du W, Hibi T, Hiraoka N, Ohta T, Ohki M, Hirohashi S, Sakamoto M. 2009. Adenylate cyclase-associated protein 1 overexpressed in pancreatic cancers is involved in cancer cell motility. *Laboratory Investigation; a Journal of Technical Methods and Pathology* **89**:425–432. DOI: https://doi.org/10.1038/labinvest.2009.5, PMID: 19188911

Yang X, Dormann D, Münsterberg AE, Weijer CJ. 2002. Cell movement patterns during gastrulation in the chick are controlled by positive and negative chemotaxis mediated by FGF4 and FGF8. *Developmental Cell* **3**:425–437. DOI: https://doi.org/10.1016/s1534-5807(02)00256-3, PMID: 12361604

Yang J, Mani SA, Donaher JL, Ramaswamy S, Itzykson RA, Come C, Savagner P, Gitelman I, Richardson A, Weinberg RA. 2004. Twist, a master regulator of morphogenesis, plays an essential role in tumor metastasis. *Cell* **117**:927–939. DOI: https://doi.org/10.1016/j.cell.2004.06.006, PMID: 15210113

Yang J, Weinberg RA. 2008. Epithelial-mesenchymal transition: at the crossroads of development and tumor metastasis. *Developmental Cell* **14**:818–829. DOI: https://doi.org/10.1016/j.devcel.2008.05.009, PMID: 18539112

Yoshioka K, Nakamori S, Itoh K. 1999. Overexpression of small GTP-binding protein RhoA promotes invasion of tumor cells. *Cancer Research* **59**:2004–2010 PMID: 10213513.,

Zhan T, Rindtorff N, Boutros M. 2017. Wnt signaling in cancer. *Oncogene* **36**:1461–1473. DOI: https://doi.org/10.1038/onc.2016.304, PMID: 27617575

Zhu X, Jiang J, Shen H, Wang H, Zong H, Li Z, Yang Y, Niu Z, Liu W, Chen X, Hu Y, Gu J. 2005. Elevated β1,4-Galactosyltransferase I in Highly Metastatic Human Lung Cancer Cells. *Journal of Biological Chemistry* **280**:12503–12516. DOI: https://doi.org/10.1074/jbc.M413631200

Zhu S, Liu L, Korzh V, Gong Z, Low BC. 2006. RhoA acts downstream of Wnt5 and Wnt11 to regulate convergence and extension movements by involving effectors Rho kinase and Diaphanous: use of zebrafish as an in vivo model for GTPase signaling. *Cellular Signalling* **18**:359–372. DOI: https://doi.org/10.1016/j.cellsig.2005.05.019, PMID: 16019189